HHS Public Access

Author manuscript

Cell Calcium. Author manuscript; available in PMC 2024 September 01.

Published in final edited form as:

Cell Calcium. 2023 September ; 114: 102770. doi:10.1016/j.ceca.2023.102770.

Understanding IP_3R Channels: from structural underpinnings to ligand-dependent conformational landscape

Mariah R. Baker[1], **Guizhen Fan**[1], **Vikas Arige**[2], **David I. Yule**[2,+], **Irina I. Serysheva**[1,+]

[1]Department of Biochemistry and Molecular Biology, Structural Biology Imaging Center, McGovern Medical School at The University of Texas Health Science Center at Houston, 6431 Fannin Street, Houston, TX 77030, USA;

[2]Department of Pharmacology and Physiology, School of Medicine and Dentistry, University of Rochester, Rochester, New York 14642

Abstract

Inositol 1,4,5-trisphosphate receptors (IP_3Rs) are ubiquitously expressed large-conductance Ca^{2+}-permeable channels predominantly localized to the endoplasmic reticulum (ER) membranes of virtually all eukaryotic cell types. IP_3Rs work as Ca^{2+} signaling hubs through which diverse extracellular stimuli and intracellular inputs are processed and then integrated to result in delivery of Ca^{2+} from the ER lumen to generate cytosolic Ca^{2+} signals with precise temporal and spatial properties. IP_3R-mediated Ca^{2+} signals control a vast repertoire of cellular functions ranging from gene transcription and secretion to the more enigmatic brain activities such as learning and memory. IP_3Rs open and release Ca^{2+} when they bind both IP_3 and Ca^{2+}, the primary channel agonists. Despite overwhelming evidence supporting functional interplay between IP_3 and Ca^{2+} in activation and inhibition of IP_3Rs, the mechanistic understanding of how IP_3R channels convey their gating through the interplay of two primary agonists remains one of the major puzzles in the field. The last decade has seen much progress in the use of cryogenic electron microscopy to elucidate the molecular mechanisms of ligand binding, ion permeation, ion selectivity and gating of the IP_3R channels. The results of these studies, summarized in this review, provide a prospective view of what the future holds in structural and functional research of IP_3Rs.

Graphical Abstract

[+]Correspondence.

Author contributions

All authors wrote the manuscript. M. R. Baker and G. Fan generated all figures; figure 6 was contributed by V. Arige and D. Yule.

Declaration of Competing Interest

The authors declare to have no competing interests.

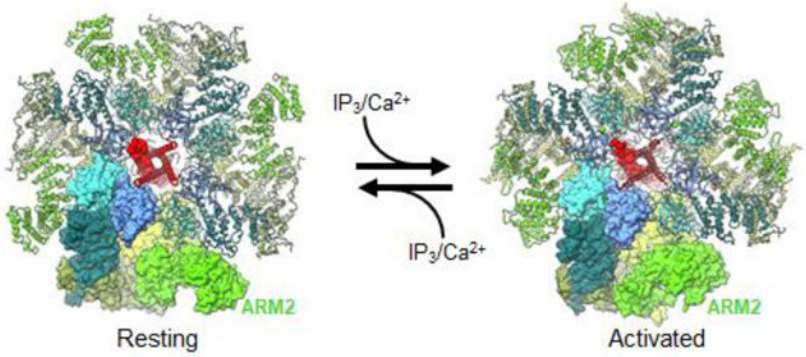

Keywords

inositol 1,4,5- trisphosphate receptors; calcium signaling; single particle cryo-EM; calcium binding sites; conformational dynamics

1. Introduction

The resolution revolution in cryogenic electron microscopy (cryo-EM) over the last decade has ushered in an explosion of structural studies of ion channels, broadening perspective and gaining insights into mechanisms of ion transport across cellular membranes. Among them are Ca^{2+} permeable ion channels, which allow calcium ions (Ca^{2+}) to flow across the lipid bilayer of cell membranes. Ca^{2+} is the most ubiquitous secondary messenger in cells. Ca^{2+} is an effective second messenger, and it is imperative that cells maintain low levels of cytosolic Ca^{2+} under resting conditions (<0.1 μM) and upon stimulation generate a temporary increase of cytosolic free Ca^{2+} in specific nanodomains. Relatively small changes in cytosolic concentration of Ca^{2+} give rise to Ca^{2+} signals that regulate a variety of cellular processes including fertilization, proliferation, differentiation, muscle contraction, neuronal signaling, and apoptosis. Most Ca^{2+} signals are due to Ca^{2+} permeable ion channels, which allow Ca^{2+} to flow across the lipid bilayer of the plasma membrane (PM) or the membranes of intracellular organelles. Inositol 1,4,5-trisphosphate receptors (IP_3Rs), the most widely expressed Ca^{2+} channels, reside in the membranes of the endoplasmic reticulum (ER) which serves as the main intracellular Ca^{2+} store.

IP_3Rs release Ca^{2+} from the ER lumen to the cytoplasm to generate Ca^{2+} signals in response to the many extracellular stimuli that evoke IP_3 formation. IP_3R-mediated Ca^{2+} signals control a vast repertoire of cellular functions ranging from gene transcription and secretion to the more enigmatic brain activities such as learning and memory. Malfunction of IP_3R signaling is implicated in numerous human diseases such as Alzheimer‟s disease, Huntington‟s disease, ataxias, heart failure, stroke and cancer [1–7]. Moreover, several disease-causing mutations have been identified in all the three IP_3R subtypes [8–12]. Consequently, efforts to understand the structure and function of IP_3R relate directly to human health and disease.

IP_3Rs are ubiquitously expressed large-conductance Ca^{2+}-permeable channels, whose opening is linked to essential phospholipase C signaling pathways that mediate the formation of IP_3 [13,14]. Complex cross-talk occurring between these pathways and IP_3R channels leads to precise regulation of intracellular Ca^{2+} levels producing cytosolic Ca^{2+} signals which differ in their spatial and temporal profiles. Versatility of IP_3-mediated Ca^{2+} signals in regulation of a broad range of cellular functions arises from the properties of IP_3Rs and their cellular organization. First, IP_3Rs open and release Ca^{2+} from the ER only when they bind both IP_3 and Ca^{2+}, the primary channel agonists. IP_3 binding primes IP_3Rs to respond to Ca^{2+}, which then promotes channel opening. Moreover, the gating of IP_3R channels is biphasically regulated by cytosolic Ca^{2+} itself. In the presence of IP_3, small elevations of Ca^{2+} enhance channel openings, whereas a further increase in intracellular Ca^{2+} causes inhibition of IP_3-evoked channel gating. Second, functional IP_3Rs are arranged in a clustered fashion on the ER membrane such that Ca^{2+} release through a single channel can trigger the opening of neighboring channels within a cluster to generate local Ca^{2+} signals, a phenomenon termed Ca^{2+}-induced Ca^{2+} Release (CICR) [15–18]. These Ca^{2+} signals propagate hierarchically in the form of Ca^{2+} blips, puffs, waves and oscillations [17,19,20]. Dual regulation by two co-agonists and clustered arrangement are key features that endow IP_3Rs with a capacity to propagate Ca^{2+} signals regeneratively between IP_3Rs as well as to other organelles (notably mitochondria, lysosomes [21,22]) and to the plasma membrane. A long outstanding question was finally resolved when the use of concatenated IP_3Rs showed that IP_3 binding to all four subunits in the tetramer is required for channel opening [23].

Besides IP_3 and Ca^{2+}, a precise spatiotemporal regulation of IP_3 R-mediated Ca^{2+} signals is achieved through regulation of IP_3R gating by other small molecules (e.g., ATP, cAMP, NADH), post-translational modifications (e.g., phosphorylation, glycosylation) and protein cofactors (e.g., Ca^{2+} sensor proteins, Bcl-2 proteins, IRBIT, Homer) [24–26]. Hence, IP_3Rs work as Ca^{2+} signaling hubs through which diverse cellular inputs are processed and then converted to cytosolic Ca^{2+} signals with precise temporal and spatial characteristics. Clearly, an in-depth understanding of the complex mechanisms through which interacting partners regulate IP_3Rs demands high-resolution structural characterization of the channel complex.

In mammals, three closely related IP_3R subtypes are encoded by different genes (ITPR1–3) from which splice variants also arise. The core properties of all IP_3Rs are similar and consistent with the sequence conservation between subtypes (~70%). Functional IP_3Rs are tetrameric assemblies (~1.3 MDa) of monomers of either identical or different subtypes, resulting in channel complexes with a wide range of functional properties *in vivo*. Early structural studies on IP_3R were focused simply on determining the correct overall structure of IP_3R, which was controversial for many years [27–31]. The first reliable structure of tetrameric full-length IP_3R1 was determined by our group to intermediate resolution (10–15 Å) in 2011 (Fig. 1) [32,33].

Over recent years, our collective knowledge of the structure and function of IP_3Rs and Ca^{2+} signals they evoke has grown considerably. There has been revolutionary progress in the cryo-EM field leading to high-resolution structures of ion channels including IP_3R Ca^{2+} channels [34–40]. In this review, we discuss recent progress in the IP_3R structure

and function that have led toward enriching our understanding of the mechanism for long-range allosteric coupling between ligand-binding and channel gating. We focus on common elements of IP_3R architecture, conformational changes and ion permeation, emphasizing mechanistic principles of gating and regulation in the family of IP_3R channels.

2. Genuine multi-modal architecture of IP_3R

After the discovery and cloning of the IP_3 receptor over four decades ago, many studies have sought to elucidate the molecular mechanisms underlying IP_3 induced Ca^{2+} release via IP_3R channels [41]. Through these years several structural techniques were utilized to characterize the structure of IP_3Rs, including X-ray crystallography, nuclear magnetic resonance (NMR) spectroscopy and single-particle cryo-EM (Fig. 1). However, to study the full-length tetrameric assembly of IP_3Rs, single-particle cryo-EM became the approach of choice due to its large size (~1.3 MDa), inherent protein flexibility, and complexities dealing with detergents in crystallization. Therefore, almost two decades ago, the low-resolution structures of the entire IP_3R1 were solved almost simultaneously by multiple groups [27–31]. However, much to the consternation of the cryo-EM and interested biochemistry communities, none of these published structures at 20–30 Å resolution agreed, even about the overall architecture of the channel. This raised the question of the credibility of single-particle cryo-EM as a tool for structural determination. The long-standing controversy about the 3D architecture of IP_3R was one of the major obstacles slowing progress of the research aiming to understand the structure-function interrelationship of this channel. The first trustworthy 3D structure of IP_3R1 was determined at ~14 Å by single-particle cryo-EM as a result of extensive work towards optimization of cryospecimen preparation [32]. Importantly, this cryo-EM structure was rigorously validated by several methods, including class-average/map comparisons, tilt-pair validation, and use of multiple refinement software packages [33]. These two key studies laid to rest a critical controversy on the IP_3R quaternary structure and provided a stepping stone for future cryo-EM studies in many groups around the world.

Merely a few short years after the validation of IP_3R1 cryo-EM structure, technical improvements to cryo-EM hardware and software aided in the burgeoning capabilities of cryo-EM to achieve near-atomic resolution structures, deemed the “resolution revolution” [42]. By harnessing these new advances, a long awaited near-atomic resolution structure of the tetrameric, full-length IP_3R1 isolated from rat cerebellum was first revealed by single-particle cryo-EM [34]. Later cryo-EM studies of recombinantly expressed human IP_3R3 protein reflected the structural conservation of the overall domain folds and assembly within the IP_3R channel family [38–40]. Currently there are multiple IP_3R1 and IP_3R3 structures of the full-length channel determined by cryo-EM in the absence (apo) or presence of regulatory molecules (*e.g.*, Ca^{2+}, IP_3, Adenophostin-A, ATP, lipids). These structures have provided valuable atomic-level insights into the complexities of the IP_3R protein machinery, the mechanisms for its regulation and how disease-causing mutations may affect channel function.

The domain architecture of the IP_3R protomer (~2700 amino acids) was first described in its entirety based on the near-atomic resolution cryo-EM structure of IP_3R1 (Figs. 2,

3) [34] and consists of large cytoplasmic (CY) assembly comprising ~90% of the protein sequence consists of two N-terminal β-trefoil domains (β-TF1 and β-TF2), three armadillo solenoid folds (ARM1-ARM3), with a helical domain (HD) inserted between ARM1 and ARM2, an intervening lateral domain (ILD) comprised of two antiparallel β sheets and two short helices, leading into the transmembrane domain (TMD) comprised of six membrane spanning alpha-helices (TM1-TM6) and two membrane associated helices (MA1-MA2). A long C-terminal helical domain (CTD) is exposed to the cytosol and connected to the TMD via the linker domain (LNK), which is sandwiched between the ILD.

The N-terminal domains, β-TF1, β-TF2 and ARM1, constitute the ligand binding domains (LBDs) with an IP_3 binding pocket formed at the cleft between β-TF2 and ARM1 in each subunit (Fig. 4) [34–40]. Cryo-EM structures of IP_3R revealed the arrangement of the N-terminal LBDs within the tetrameric channel assembly. The β-TF1, β-TF2 and ARM1 domains within each IP_3R subunit form a triangular assembly, similar to that seen in crystal structures [44–46] and constitute an apical portion of the cytoplasmic solenoid that encircles the CTD bundle.

Multiple positively charged conservative residues from β-TF2 and ARM1 are involved in coordinating IP_3 in the binding pocket in all three IP_3R subtypes (Fig. 4). Upon binding IP_3 there is ~4 Å closure of the cleft caused by a shift of the ARM1 domain toward the β-TF2 domain to allow for the coordination of the IP_3 molecule. It has been found that mutations causing cerebellar ataxia are located within or near the IP_3-binding pocket of IP_3R1, and these pathological mutations either impair IP_3 binding or disrupt channel gating without affecting IP_3 binding [43].

The β-TF1 domain is not directly involved in the formation of the IP_3 binding pocket, but it reduces the affinity of IP_3 binding [47]. The lack of the β-TF1 results in inhibition of IP_3-induced Ca^{2+} release although this mutant IP_3R1 had 10-times higher IP_3-binding affinity than the wild type. Thus, this N-terminal domain was referred to as a suppressor domain (SD). The β-TF1 forms intra-subunit interfaces with the β-TF2 and ARM1 domains, as well as interacts with the β-TF2, ARM2 and ARM3 domains from the neighboring subunit. It was reported that the β-TF1 loop comprising residue Y167 (‘hot spot’) is essential for the Ca^{2+} release activity of IP_3Rs [48] and is located at the inter-subunit β-TF1-β-TF2 interface which undergoes conformational changes upon binding of adenophostin A (a structural analog of IP_3) [35]. Collectively, these data suggest that the β-TF1 domain might be important for stabilizing inter-domain interactions and plays an important role in coupling ligand-binding signals to channel opening. In addition, a helix-loop-helix structure (so called the ‘handle’ of the hammer-shaped SD) of the β-TF1 projects inward into the hollow solenoid of the channel and interacts with the ARM3 domain from the neighboring subunit. It was demonstrated that deletion of the handle does not affect IP_3-mediated channel activation [48]. This justifies the structure-stabilizing role of the β-TF1-ARM3 interaction. Our recent progress with analysis on how ligand-binding signals might be communicated within the conformational protein landscape are discussed in the section below.

Of note, ryanodine receptors and IP_3Rs share a modest ~20% sequence identity within their first ~700 residues [50]. Upon the determination of structures for both channels, the

protein folds appear nearly identical for the N-terminal region [49]. A cleft between the RyR domains NTD-B and Nsol, equivalent to the β-TF2 and ARM1 domains in IP_3Rs, exists and is similar to the IP_3 binding pocket in IP_3Rs (Fig. 4). However, in RyR1 the residues within this cleft form a negative surface charge in contrast to the positively charged surface in IP_3Rs that contributes to IP_3 binding and underlies the rationale for why RyRs do not bind IP_3 [50].

The Ca^{2+} conduction pathway is formed in the tetrameric assembly of the channel along the central four-fold axis. The TM5 and TM6 helices form a right-handed pore bundle shaping the ion conduction pathway. The TM1-TM4 connect to the pore-forming bundle through a lateral TM4-5 amphipathic helix, which allows for a domain swapped configuration of the TMDs whereby the TM1–TM4 bundle of one subunit interacts with the pore forming helices from the neighboring subunit. This domain swapped architecture is a highly conserved structural feature for many tetrameric cation channels. The luminal entrance of the ion conduction pathway harbors the P-helix and P-loop containing the selectivity filter sequence (GGVGD) and a ring of hydrophobic side chain residues F2586 and I2590 from the TM6 helices form a constriction site in the closed channel that can prevent the flow of Ca^{2+} ions across the membrane bilayer. The G2498S mutation in the selectivity filter was found to be associated with anhidrosis in humans and abolished Ca^{2+} releasing activity in the IP_3R2 channel [51].

Lipids are integral to structure and function of ion channels residing in a lipid membrane bilayer *in vivo*. Recent cryo-EM studies revealed lipid molecules bound to the TM helices in IP_3R1, suggesting conserved locations of protein-bound lipids among homo-tetrameric ion channels [36]. However, the exact molecular mechanism by which lipids exert their effects on the IP_3R channel remains to be elucidated.

In the tetrameric assembly, the α-helical distal portion (residues 2692–2737) of the CTD (Fig. 2) from each protomer forms a central, left-handed helical bundle, and the CY domains are constructed around this CTD bundle to form α-helical solenoid modules, well adapted for binding multiple ligands and protein-protein interactions. Noteworthy, the N-terminal β-TF2 domain makes an inter-subunit interface with the α-helical CTD from the neighboring subunit [34–37]. Thus, the entire tetrameric IP_3R assembly is uniquely arranged around two helical bundles: a ~70 Å left-handed CTD α-helical bundle is connected to the right-handed α-helical TM6 bundle via the ILD/LNK domains lying at the CY-membrane interface. The allosteric nexus formed by ILD and LNK domains represents the sole direct structural link between the CY and TM domains.

It is notable that both IP_3R1 and IP_3R3 exhibit identical overall architectural arrangements (Fig. 3). However, in IP_3R3 structures the central coiled-coiled CTD α-helical bundle is not resolved [38–40], yet based on studies of IP_3R1 the CTD bundle is one of essential elements for maintaining structural integrity of the channel assembly and for transmitting ligand-evoked signals from LBDs to the ion-permeation pore [34–37]. This view is consistent with functional $IP_3R1\text{-}TM_{RyR}$ chimeras [46] since the RyR structure does not have an extended CTD, the reduced efficacy of IP_3 suggests that within $IP_3R\text{-}TM_{RyR}$, communication between the N-terminal β-TF2 and channel are less effective than in native IP_3R1, and with the

evidence that IP_3R1 function is lost when more than 43 residues are deleted from the C-terminus [52]. It is conceivable that the methods used for expression and purification of recombinant IP_3R3 yielded the channel lacking the structural coupling between the LBDs and TMDs underlying the activation mechanism in IP_3Rs due to compromised structural integrity of the tetrameric channel assembly. Another remote possibility is that different IP_3R subtypes might explore different mechanisms for allosteric regulation of the channel activity given differences in the lengths and sequences of their C-terminal tails (Fig. 2).

While structural studies of IP_3R2 have yet to be performed, a predicted molecular model generated using Alphafold2 [53] suggests that the subtype 2 receptor shares a similar domain architecture as defined for subtypes 1 and 3 (Figs. 2, 3). Moreover, overall comparison of IP_3Rs and RyRs, the two related families of Ca^{2+} release channels, parallels many structural and functional properties in both families, and there has been fruitful synergy between the research on these important ion channels (Figs. 2, 3) [41,49]. Thus, the emerging concept for the versatility of Ca^{2+} signaling via Ca^{2+} release channels is founded in the distinctive structure of IP_3Rs. In this context, IP_3R channels can be viewed as having highly dynamic scaffolding, where binding of multiple ligands and modulatory molecules alters the conformational landscape of protein and propagates ligand-evoked signals to the channel pore.

3. Ca^{2+} binding diversifies the conformational ensemble of IP_3R

A functional hallmark of IP_3R channel gating is its biphasic regulation by Ca^{2+} in the presence of activating concentrations of IP_3, with low Ca^{2+} concentrations promoting channel activation and higher Ca^{2+} concentrations inhibiting the channel [54–56]. These observations suggest the presence of at least two functional Ca^{2+} binding sites in IP_3R with different Ca^{2+} affinities – a high affinity Ca^{2+} binding site to allow for Ca^{2+} activated release and a low affinity Ca^{2+} binding site that can inhibit Ca^{2+} release [57]. While the binding of both IP_3 and Ca^{2+} are required for channel activation, the exact mechanism of their interplay and how these co-agonists transmit the gating signal, as well as how Ca^{2+} binding can lead to inhibition has not been well understood. In the primary sequence, IP_3Rs lack any canonical Ca^{2+} binding motifs such as an EF-hand or C2 domain, which has made identification of Ca^{2+} binding sites complicated [58]. Yet, purified IP_3Rs reconstituted into lipid bilayers are regulated by Ca^{2+} in a biphasic manner strongly indicating that the IP_3Rs have intrinsic Ca^{2+} binding site/s [59].

Recently, insights into Ca^{2+} regulation of channel gating have been advanced by structural studies of full-length, tetrameric IP_3Rs by single-particle cryo-EM and validated with functional studies [37,60]. Cryo-EM studies of IP_3Rs determined in the presence of Ca^{2+} have identified Ca^{2+} binding sites within the channel in conditions to promote capturing the channel in physiologically relevant states (Supplementary Figs. 1 and 2). In IP_3R1 five Ca^{2+} binding sites per monomer were identified, three in the cytosolic LBD and Ca^{2+}-sensor (S) domains ($Ca\text{-}I_{LBD}$,$Ca\text{-}II_{LBD}$, $Ca\text{-}III_S$) and two within the ion conduction pathway (Ca-IV, Ca-V) (Fig. 5). In IP_3R3 two sites have been described, Ca-CD and Ca-JD, the latter of which is equivalent to $Ca\text{-}III_S$ in IP_3R1. In IP_3R1, two Ca^{2+} binding sites were identified within the apical ligand binding domains, one at the intersubunit interface of β-TF1 and

β-TF2 from neighboring subunits (Ca-I_{LBD}) and the second formed at the intra-subunit interface between the β-TF1-β-TF2 domains (Ca-II_{LBD}). In Ca-I_{LBD} the Ca^{2+} is coordinated by carboxyl groups from the negatively charged D426 and D180 residues in βTF2 and βTF1 domains, respectively. Ca-II_{LBD} utilizes the oxygen atoms from the E283 side chain and backbone oxygen atoms from the surrounding βTF1 domain residues to coordinate Ca^{2+}. The location of the Ca-I_{LBD} and Ca-II_{LBD} sites are consistent with predicted Ca^{2+} binding sites [44,61]. The third cytosolic Ca^{2+} binding site, Ca-III_S, is located at the interface between the ARM3 and LNK domains and is comprised of the acidic E1978, E2042 (ARM3 domain) and T2654 (LNK domain) residues in IP_3R1. Ca^{2+} binding to the Ca-III_S site has also been observed in two IP_3R3 cryo-EM structures. Moreover, cryo-EM structures of RyR1 in the presence of Ca^{2+} have also shown that conserved residues in the structurally homologous region of RyR1 also serve to coordinate Ca^{2+} (Fig. 5). Mutations in the residues constituting the Ca^{2+} binding pocket in RyR1/2 are the underlying cause of central core disease and arrhythmogenic diseases [62–64]. The Ca^{2+} binding sites, Ca-IV and Ca-V, were identified within the luminal side of the ion conduction pathway and may represent high affinity ion binding sites for the Ca^{2+} ion as the ion passes from the ER lumen to the cytosol. These sites could be involved in luminal regulation of the channel, however, their functional role remains to be established.

An additional Ca^{2+} binding site (Ca-CD) in IP_3R3 has been proposed at the interface between HD and ARM2 domains (CLD domain in IP_3R3 structure) in based on the cryo-EM structure of IP_3R3 in the presence of 2 mM Ca^{2+}. In order to form the Ca-CD site, it is necessary for the ARM2 domain to adopt a retracted conformation, moving ~30 Å toward the HD and reducing the inter-subunit contacts between ARM2 and β-TF1 from the neighboring subunit. Supporting the Ca^{2+} coordination within this site are main-chain oxygens atoms from R743 (HD) and E1122 (ARM2) and side chain atoms from E1125.

Several structures of IP_3Rs have now been determined by cryo-EM in the presence of Ca^{2+} and have been observed to adopt a similar retracted conformation of ARM2 (Figs. 5, 8), yet only one group has reported Ca^{2+} binding site in this domain [38]. Moreover, in other IP_3R3 cryo-EM structures, as well as in IP_3R1, the domains comprising the Ca-CD site have not been sufficiently resolved to confidently detect the bound Ca^{2+} ion at this location [37,40]. It was also demonstrated that the same region in IP_3R1 is highly dynamic exhibiting significant motions [37].

The Ca^{2+} bound IP_3R1 structures were obtained in different Ca^{2+} and ligand combinations to better understand the role of Ca^{2+} during channel gating and inhibition. In the IP_3R1 structure determined in the presence of an inhibitory Ca^{2+} concentration (20 μM), the five Ca^{2+} binding sites were occupied, while at 2 μM Ca^{2+} in the presence of IP_3 and ATP, four Ca^{2+} binding sites were occupied. Ca^{2+} was not seen in the Ca-I site under lower Ca^{2+} conditions, indicating this site could have a lower apparent affinity for Ca^{2+} than the other Ca^{2+} binding sites.

It has been proposed that binding of IP_3 serves to alter the Ca^{2+} regulation of the channel, whereby IP_3 allosterically regulates Ca^{2+} inhibition without affecting Ca^{2+} activation [65–67]. In the light of the Ca^{2+} binding sites described for IP_3R1 obtained at low and high

Ca^{2+} concentrations, the Ca-I_{LBD} site may potentially play a role in Ca^{2+} inhibition of IP_3R1. Conformational changes within the Ca-I_{LBD} binding site suggest that IP_3 regulates the conformation of the Ca-I_{LBD} site. However, based on current available structures, the impact of IP_3 binding on the Ca-I_{LBD} at inhibitory Ca^{2+} concentrations is an outstanding question. Functional studies of Ca-I_{LBD} would be necessary to address its role in Ca^{2+} dependent inhibition. It has also been suggested that the IP_3R3 Ca-CD site plays a role in Ca^{2+} inactivation, however, further structural and functional characterization is still needed to address the role of this site in IP_3Rs.

There has long been a search for the Ca^{2+} binding site/s necessary for Ca^{2+} activation of the IP_3R channels. A previous candidate for a functional Ca^{2+} binding site was E2101. However, mutations of this residue in IP_3R1 altered both the Ca^{2+} dependent activation and inhibition of channel activity [68,69]. Cryo-EM structural analysis revealed that this residue is not involved in coordinating Ca^{2+} but may have an ancillary role in favoring Ca^{2+} binding to the Ca^{2+}-sensor (Ca-III_S). The Ca-III_S binding site was shown to be occupied under activating and inhibitory Ca^{2+} conditions and mutations to the analogous site in RyR1 altered Ca^{2+} activation of the channel [70]. However, the functional role for the Ca-III_S site was unknown for IP_3R channels. Through mutagenesis and electrophysiological studies, we have now demonstrated that the Ca-III_Ssite is responsible for Ca^{2+} activation in IP_3R1 and IP_3R3. Mutation of the conserved acidic residues within the Ca-III_S binding site in subtype 1 and subtype 3 IP_3R resulted in Ca^{2+}-dependent activation being significantly diminished or abrogated without altering the Ca^{2+}-dependent inhibition (Fig. 6) [60]. Neutralizing the negative charge on the side chain residues dramatically shifted the Ca^{2+} dependency to a higher concentration. Importantly, the Ca-III_S mutations did not compromise the tetrameric integrity and proper localization of IP_3Rs. Moreover, the Ca-III_S site is occupied in the presence and absence of IP_3 indicating that access to the activating Ca^{2+} site is not regulated by IP_3. The originally targeted putative Ca^{2+}-sensor residue, E2101, affected both activation and inhibition of the channel, indicating that it plays an allosteric role in channel regulation. Based on cryo-EM structures, the E2101 residue is nearby, but outside of the Ca-III_S binding pocket and it can likely form a hydrogen bond with neighboring residues within the ARM3 domain. Thus, mutation of E2101 and the analogous residues in IP_3Rs/RyRs could disrupt the ability to maintain the structural fidelity for the Ca-III_S binding site and signal transmission to the TM6 gating helix [37].

The residues involved in the Ca^{2+} coordination of Ca-III_S are conserved in both RyRs and IP_3Rs and the functional and structural observations strongly indicate that the Ca^{2+} activation site is evolutionarily well conserved and a common underlying mechanism that governs both IP_3Rs and RyRs channel activation (Fig. 5). Mechanistically, Ca^{2+} binding to the activation site may facilitate conformational changes in IP_3R structure, promoting pore opening. However, it is still not clear whether Ca^{2+} binding is cooperative and if all the stimulatory/inhibitory Ca^{2+} binding sites must be occupied for channel opening/closure. Future experiments using concatenated receptors with one or more subunits of a tetramer harboring mutations at the Ca^{2+} binding sites will address the precise stoichiometry.

4. Allosteric nexus as a structural platform for transmitting ligand-evoked signals

The allosteric nexus is a critical junction between the cytoplasmic and transmembrane domains that serves to process and transmit the ligand-dependent regulatory signals from the cytosolic domains to the channel gating apparatus. This occurs through the intra-subunit assembly of the ILD and LNK at the membrane-cytosol interface. It has recently been shown that besides a conserved Ca^{2+}-binding site (Ca-III_S), which utilizes residues from the ARM3 and LNK domains connected to the nexus, the nexus carries binding sites for zinc and ATP [36–38,40].

While it remains to be established how a conformational wave generated upon binding of the activating ligands propagates from the LBDs in the apical portion of the CY scaffold to the ILD/LNK (‘nexus’) assembly, cryo-EM structures clearly revealed that upon binding of activating ligands the allosteric nexus undergoes lateral and rotational movements that result in dilating the nexus assembly. These conformational changes appear to impose the impetus that allow to reconfigure the connected TM helices that leads to opening of the channel gate [35,37].

Recent studies provided evidence confirming activating function of the Ca-III_S site located at the ARM3 domain connected to the ILD [60]. In addition, it was reported that the Ca-III_S site undergoes IP_3-induced conformational changes and this leads to activation of the channel gating [38,40]. However, this notion is not supported by studies of IP_3R1 showing that the Ca-III_S site does not change between apo-, Ca^{2+}- and IP_3-bound structures of IP_3R1 [37].

Adenine nucleotides are known to bind IP_3Rs and can enhance IP_3-induced Ca^{2+} release in a concentration dependent manner. All three IP_3R subtypes bind ATP with varying affinities, ranging from low micromolar to millimolar levels [71–73]. The addition of ATP in the presence of channel activators, IP_3 and Ca^{2+}, in single channel studies revealed that ATP increased the channel open probability without affecting channel conductance [55]. Binding of ATP is proposed to tune the sensitivity of the IP_3R channel to activating Ca^{2+}. ATP concentrations in the cell stay relatively high and constant (> 1mM) and as such ATP may remain constitutively bound to enhance Ca^{2+} release upon receptor stimulation. It has however been proposed that ATP^{4-}, an ATP derivative in neutral solution, is essential for regulation of IP_3R-induced Ca^{2+} release [74], and because the levels of this form of ATP are in the micromolar range, a possibility exists that IP_3Rs are dynamically regulated by changes in ATP concentrations. In addition, many studies have demonstrated that the mitochondria and ER are in close proximity in many cells types, thus release of ATP from mitochondria in close proximity to IP_3R and regulation of the IP_3R-mediate Ca^{2+} release by ATP may have significance for intracellular signaling by providing a cross-talk between the mitochondria and the ER [75–77].

In the search for the molecular determinants necessary for ATP binding and potentiation of channel activation, several canonical ATP binding motifs (GXGXXG) were identified within the IP_3R primary sequence (ATP-A:2016–2021 in IP_3R1 S2+ and IP_3R3; ATP-B site:1773–

1780 in IP_3R1 S2+, and ATP-C:1688–1732 in IP_3R1 S2−). All three putative ATP-binding sites were shown to bind ATP in recombinantly expressed fragments, however, amino acid substitutions within the motifs did not alter ATP regulation of IP_3R1 or IP_3R3 subtypes indicating that ATP modulates IP_3R-mediated Ca^{2+} release by binding to a region distinct from the glycine-rich motifs [78–80].

Cryo-EM studies of IP_3R1 and IP_3R3 proved crucial to delineating the ATP binding site. Structures of IP_3Rs in the presence of saturating ATP concentrations were solved by cryo-EM to better than 3.5 Å resolution allowing for the accurate model building for protein side-chains and identification of the ATP binding site [37,40]. In the presence of ATP, strong cryo-EM densities were observed at an interfacial region between the cytoplasmic and TM domains and could accommodate an ATP molecule. One bound ATP per IP_3R subunit was identified and is consistent with Scatchard analysis [81].

The ATP binding pocket is formed at an interface of two domains, ILD and LNK, from the same subunit, and adjacent to the cytosolically exposed end of the TM6 helix. The binding pocket is electrostatically favorable for accommodating the negatively charged phosphate tail through a series of lysine residues from ILD and LNK domains while the adenine moiety is predominantly surrounded by hydrophobic residues (Fig. 7).

There are little observed conformational changes within the ATP binding pocket between ATP-bound and apo-state structures of IP_3R, however the ATP binding site is located at a critical junction between cytoplasmic and transmembrane domains, termed the allosteric nexus. The ATP binding site is in a unique position to impart a structural/allosteric effect in synergy with the activating Ca^{2+} binding site ($Ca\text{-}III_S$) located in the nearby ARM3 domain to potentiate channel openings. The ATP interactions with IP_3R1 may stabilize domains to amplify the effects of Ca^{2+} binding on the gating of the channel pore, thus increasing the apparent affinity of Ca^{2+} needed to activate the channel consistent with single channel studies [82].

While the structural fold of the ATP binding pocket is conserved among IP_3Rs, subtle differences in amino acid composition result in differences on the charged surface of the binding pocket with IP_3R1 having greater positively charged surface area available for interaction with the ATP phosphates than observed in IP_3R3 (Fig. 7). This is consistent with the much higher affinity for ATP reported for IP_3R1 than IP_3R3. Of note, sequence alignment of positively charged, polar lysine residues in IP_3R1 at 2221, 2224, 2633 positions which are identified to interact with the ATP triphosphate tail [37,40] revealed the K2224 and K2633 are conserved in all the three IP_3R subtypes. Surprisingly, the K2221 in IP_3R1 aligns with a positively charged, polar arginine (R) in IP_3R2 and a negatively charged, polar glutamic acid (E) in IP_3R3 which could perhaps contribute to the previously reported higher sensitivities of IP_3R1 and IP_3R2 to ATP as compared to IP_3R3.

Moreover, the ATP binding pocket appears to be a conserved feature between IP_3Rs and RyRs indicating that a similar underlying mechanism may prime these channels to ATP potentiation [37]. RyR channel activity is also potentiated by ATP binding, and the ATP-binding site has been identified at the interface between the thumb and forefinger (TaF)

domain and CTD, which are structurally equivalent to the ILD and LNK domains in IP_3Rs. However, in RyR1 ATP adopts a slightly different binding position with the phosphate tail pointed toward the membrane plane while in IP_3Rs it lies more parallel to the membrane plane. The difference in orientation of ATP in RyR may be due to an additional positively charged residue (R4215) that can coordinate with the phosphate tail that is not observed in IP_3Rs. Recent mutagenic analysis of residues within the RyR1 ATP binding pocket supports that this ATP binding site is responsible for regulating Ca^{2+} release from RyR1 and linked to myopathies in humans [83].

Adjacent to the ATP binding domain is the C2H2-like zinc-finger domain composed of amino acids from the LNK domain (C2611, C2614, H2631, H2636 in IP_3R1; C2538, C2541, H2558 and H2563 in IP_3R3; and C2562, C2565, H2582, H2587 in IP_3R2) and the resolution of the IP_3R1 and IP_3R3 cryo-EM density maps are sufficient to model one bound zinc molecule per subunit. An equivalent Zn^{2+}-finger domain was also described for RyRs in its CTD, which is structurally analogous to the IP_3R LNK domain (Fig 7). Mutations to the conserved cysteine or histidine residues necessary for tetrahedral coordination of the Zn^{2+} molecule were shown to either inhibit or abolish IP_3-induced Ca^{2+} release without affecting IP_3 binding to the IP_3R1 and abolished the response of RyR to caffeine activation [47,84]. While there is some indication that RyR2 may be regulated by Zn^{2+} [85], evidence for physiological regulation of IP_3Rs by Zn^{2+} has not been established. Given the proximity of the LNK domain to the TMDs and regulatory ligand binding sites, this zinc-binding domain clearly has an important role in influencing channel gating. It is of note that in all cryo-EM studies of IP_3Rs to date that have identified bound Zn^{2+} ions, the buffer solutions have also included the high-affinity cation chelators EDTA and/or EGTA suggesting that Zn^{2+} is either a constitutively associated cation with a high binding affinity or that the concentration of contaminating Zn^{2+} is beyond the capacity of the buffering solutions.

5. Dynamic conformational landscape of IP_3R as a basis for multi-modal regulation

IP_3R channels integrate numerous regulatory inputs including Ca^{2+} levels in the cytosol and ER lumen, ATP binding, protein phosphorylation and thiol modifications to alter channel function and fine tune the Ca^{2+} signal. However, ultimately the activation of IP_3R relies upon an intricate interplay of its primary ligands, IP_3, Ca^{2+}, to initiate a structural rearrangement within the channel architecture to allow for Ca^{2+} to move across the ER membrane via a chemical gradient into the cytosol. It is obvious that channel functionality greatly benefits from the modular solenoid arrangement of the CY domains which flexibility allows IP_3Rs to accrete many auxiliary modulatory proteins *in vivo* [24]. In cryo-EM, the protein sample, trapped within vitreous ice under particular buffer conditions, is captured in discrete static conformations, and with sufficient number of particles, computational sorting can retrieve informative structural details about these conformations. However, there is a gap between the high-resolution structural snapshots of the channel and functional studies demonstrating different levels of IP_3R channel activity even under constant experimental conditions. Clearly, to derive functionally relevant connections between high-resolution

snapshots, there is a pressing need for analysis of ligand-dependent dynamic conformational landscape of the channel protein.

Recently, new deep-learning based methods of manifold analysis have allowed for the extraction of protein dynamics, effectively generating molecular movies for the trajectories of macromolecular movements based on experimental cryo-EM 2D data without any structural interpolations [86–90]. By harnessing the computational power of deep-learning neural network approach [87] and 3D variability analysis [89], molecular motions of the IP_3R1 protein were extracted directly from cryo-EM density data [37]. These data revealed that the ARM2 domain in IP_3R1, comprising the peripheral cryo-EM densities of the cytoplasmic scaffold, exhibits an intrinsic flexibility, exploring motions between an extended or retracted conformation (Fig. 8). In the extended conformation, the ARM2 domain from one subunit makes extensive contacts with β-TF1 and ARM1 domains from the neighboring subunit. While in the retracted conformation the inter-subunit contacts are significantly reduced because the ARM2 domain retracts ~30 Å away from the neighboring subunit and shares only a minimal interface with the β-TF1 domain. We found that unliganded (apo) and high Ca^{2+} IP_3R1 structures exhibited the ARM2 domain preferentially in the extended conformation, while the IP_3R1 structure determined in the presence of IP_3, ARM2 was predominantly observed in the retracted conformation (Fig. 8).

The same motion trajectories for the ARM2 were observed for all three states (apo, Ca^{2+}-bound and Ca^{2+}/IP_3/ATP-bound IP_3R1s), however the amplitude of motion towards the retracted conformation increased in the presence of IP_3 [37]. Based on these observations, we conclude that IP_3-binding process in the tetrameric channel is coupled to conformational motions of the ARM2 domain, and exhibits a mechanism similar to a ‘reversible ratchet’ where ARM2 (“gear”) switches back-and-forth between ‘extended’ and ‘retracted’ conformations with the extended conformation restrictive for IP_3 binding and retracted conformation suitable for capturing IP_3 due to release of structural constraints at ARM2-βTF1 and ARM2-ARM1 interfaces between the neighboring subunits (Fig. 9).

The ARM2 anchors the inter-subunit LBD interfaces thereby restricting the IP_3-binding domain dynamics that is required for capturing the ligand (Fig. 8). Furthermore, in the IP_3R lacking the β-TF1 domain the IP_3-binding pocket will display a higher degree of dynamics that correlates with observed higher IP_3-binding affinity [47]. And as such, we propose that the characteristic motions of the ARM2 and the correlated flexibility of the IP_3-binding pocket might define isoform-specific affinity of IP_3Rs. This explains why the N-terminal βTF2-ARM1 expressed and isolated as individual entities from all three IP_3R subtypes bind IP_3 with similar affinity, yet the full-length receptors display different affinities to IP_3 (IP_3R2>IP_3R1>>IP_3R3) despite conservation of the IP_3-coordinating residues across the IP_3R subtypes. It is conceivable that IP_3R subtypes exhibit different conformational dynamics underlying subtype-specific IP_3-binding.

The retracted and extended forms of ARM2 have also been observed in cryo-EM structures of IP_3R3s, where the predominant class of particles produces a cryo-EM structure in the unliganded state with ARM2 in the extended form. In the presence of channel activators and with multiple finely separated 3D classes, one small class of particles resulted in the

ligand-bound activated channel with ARM2 in the retracted conformation, consistent with retracted conformation seen in IP_3R1 [40]. A third structure has also been observed to contain the retracted ARM2 [38], but is not consistent with the high Ca^{2+} (20 μM) structure of IP_3R1. The extreme Ca^{2+} concentration (2 mM Ca^{2+}) may account for the differences observed.

With multiple cryo-EM structures of IP_3Rs determined under different conditions (Supplementary Figs. 1 and 2), the structural underpinnings toward IP_3R activation and inhibition have begun to emerge (Fig. 9). In the tetrameric channel the role of the dynamic ARM2 is attributed to weakening inter-subunit interactions with βTF1 and ARM1 domains which allows the IP_3-binding pocket to explore multiple conformations including the conformation capable of capturing IP_3.

Based on several proposed structures of IP_3R3 in the ‘inactive state’, it is observed that at high (~2 mM) Ca^{2+}, the cytosolic subunits of the channel splay away from the central 4-fold axis [38,40]. The observed ~30 Å dilation of the LBD ring leads to a disruption of the inter-subunit interfaces and loss of structural integrity of the cytosolic scaffold. These structures raise a serious question about their physiological relevance. It becomes difficult to conceive what it would take to reconfigure the channel from such extreme–conformation to the conformation susceptible to binding of activating ligands? Another possibility is that the observed ‘inactive’ conformation reflects a detrimental disintegration of the tetrameric channel assembly under chosen experimental conditions. Further rigorous analysis of the channel conformational landscape combined with high-resolution structural determination and functional studies is needed to reconcile these observations and to establish a functional path of structural changes underlying communication of ligand-evoked signals toward channel activation and inhibition.

6. Perspectives

With the “resolution revolution” in cryo-EM, the picture of IP_3R channel gating and its multi-modal regulation seems to be developing in a straightforward manner, however, many fundamental questions still remain unanswered which curtail our understanding of the molecular mechanisms governing control of IP_3R-mediated Ca^{2+} signaling: What is the structural basis for functional coupling between the ligand binding domains during IP_3/Ca^{2+}-mediated channel gating? Does the binding of Ca^{2+} to the sites identified in the cryo-EM structures underpin the biphasic regulation of IP_3R by Ca^{2+}? How does the unique IP_3R architecture contribute to channel modulation by an array of regulatory proteins? What is a structural basis of isoform-specific properties of three members of the IP_3R family? How are IP_3Rs assembled into clusters on ER membranes?

Recent near-atomic resolution structures of IP_3R1 and IP_3R3 determined in the apo- and several ligand-bound states revealed common elements of the channel architecture and now begin to provide important insights into the molecular mechanisms of dual activation of the channel by IP_3 and Ca^{2+}. However, many structural details are still missing due to insufficient local resolution that includes side-chain placements in some parts of the protein, conformations of flexible loops, ions and water. Of note, 13% and 20% of the protein

backbone is not resolved in IP_3R1 [37] and IP_3R3 structures [38,40], respectively, including phosphorylation sites and other intrinsically flexible or disordered regions. Noteworthy, while both IP_3R1 and IP_3R3 exhibit similar architectural arrangements, the helical bundle formed by the *C*-terminal domains in IP_3R1 is not resolved in the IP_3R3 cryo-EM maps to make definitive conclusions about the conformational changes underlying ligand-binding and gating activation, which may be conserved among IP_3R subtypes. Each of these channel subtypes has unique gating properties, and in many instances, different subtypes assemble as heterotetrameric complexes to form the native IP_3R channel *in vivo*. However, due to the lack of high-resolution structure of IP_3R2, subtype specific gating and modulation remain largely incomplete.

Compositional and conformational variability among particles in single-particle analysis remains a key challenge for the field. Approaches such as classification have been around for decades [91–93], and partially address the issue by at least providing a handful of stable states, but do not fully characterize the full particle variability available from the particle population in the vast majority of cases. Single-particle cryo-EM studies have reported that the IP_3R structure undergoes conformational changes upon ligand binding [35–40], suggesting structural flexibility of IP_3R that allows the channel to switch from a closed state, capable of interacting with its ligands, to an open state, capable of transferring Ca^{2+} ions across the ER membrane.

However, all these 3D cryo-EM structures represent snapshots of defined static channel conformations, and the mechanistic insights are derived based on interpolations between discrete structures, each of them likely a mixture of states from a dynamic conformational ensemble. It is clear that the large IP_3R assembly comprising multiple flexible domains undergo complex dynamics with entropy and transitory ligand binding as the only driving factors. Thus, rather than triggering a discrete change of state, ligand binding instead alters the entropic neighborhood of conformations naturally explored by the channel. This leads to a large number of continuously varying conformations. Through use of deep learning methods implemented in the cryo-EM field [86–90,94], recent studies of IP_3R1 were able to simultaneously characterize conformational variability and structure on the channel [37], providing a structural mechanism (‘reversible ratchet’) for the susceptibility of IP_3R to binding of IP_3, based on the conformational selection of the ligand-binding pocket, which may adapt different conformations in its unbound state for which IP_3 binds selectively to one of these conformations. From this study, we can see now that instead of directly going from closed to open conformation, the pore-forming elements can adopt a mixture of conformations resulting in different levels of channel activity observed under constant experimental conditions in electrophysiological studies. The dynamics of IP_3R *in vivo* is extremely complicated given that the channel function is regulated by an array of modulatory molecules, ranging from ions, small chemical compounds and lipids to protein cofactors that shape the amplitude, timing, and duration of IP_3R-mediated Ca^{2+} signals [24,25,95]. Although high-resolution structural knowledge of all three subtypes of IP_3R channel is essential to gain an in-depth mechanistic understanding of IP_3R function, high-resolution structures can be biased by stabilizing measures such as ligands, mutations, leaving open questions as to the native activation process. Use of deep learning-based methods to analyze cryo-EM images can yield a distinct view of conformations that may be

refractory by traditional high-resolution single-particle approach. Further systematic work combining analysis of the dynamic conformational landscape of IP_3R with site-directed mutagenesis and electrophysiological characterization will be needed to test connections between protein motions and functional paths underlying transfer of ligand-mediated allosteric information within the channel.

Supplementary Material

Refer to Web version on PubMed Central for supplementary material.

Acknowledgements

This work was supported by grants from the National Institutes of Health (R01GM072804 to I.I.S.; DE019245 to D.I.Y.), Welch Foundation research grant (AU-2014-20220331 to I.I.S.) and American Heart Association grant (23CDA1048883 to G.F.)

References

[1]. Jacobsen AN, Du XJ, Lambert KA, Dart AM, Woodcock EA, Arrythmogenic action of thrombin during myocardial reperfusion via release of inositol 1,4,5-triphosphate. Circulation. 93 (1996):23–26. [PubMed: 8616935]

[2]. Marks AR, Intracellular calcium-release channels: regulators of cell life and death. Am J Physiol. 272 (1997):H597–605. [PubMed: 9124414]

[3]. Matsumoto M, Nakagawa T, Innoe T, et al. , Ataxia and epileptic seizures in mice lacking type 1 inositol 1,4,5-triphosphate receptor. Nature. 379 (1996):168–171. [PubMed: 8538767]

[4]. Hetts SW, To die or not to die: an overview of apoptosis and its role in disease. JAMA. 279 (1998):300–307. [PubMed: 9450715]

[5]. Perry G, Nunomura A, Lucassen P, Lassmann H, Smith MA, Apoptosis and Alzheimer's disease. Science. 282 (1998):1268–1269. [PubMed: 9867630]

[6]. Thompson CB, Apoptosis in the pathogenesis and treatment of disease. Science. 267 (1995):1456–1462. [PubMed: 7878464]

[7]. Bezprozvanny I: Inositol 1,4,5-tripshosphate receptor, calcium signalling and Huntington's disease, vol 45. Edited by Harris JR: Springer; 2007.

[8]. Terry LE, Alzayady KJ, Furati E, Yule DI, Inositol 1,4,5-trisphosphate Receptor Mutations associated with Human Disease. Messenger (Los Angel). 6 (2018):29–44. [PubMed: 30197841]

[9]. Kerkhofs M, Seitaj B, Ivanova H, Monaco G, Bultynck G, Parys JB, Pathophysiological consequences of isoform-specific IP(3) receptor mutations. Biochim Biophys Acta Mol Cell Res. 1865 (2018):1707–1717. doi: 10.1016/j.bbamcr.2018.06.004. [PubMed: 29906486]

[10]. Terry LE, Arige V, Neumann J, et al. , Missense mutations in inositol 1,4,5-trisphosphate receptor type 3 result in leaky Ca^{2+} channels and activation of store-operated Ca^{2+} entry. iScience. 25 (2022):105523. doi: 10.1016/j.isci.2022.105523. [PubMed: 36444295]

[11]. Terry LE, Alzayady KJ, Wahl AM, Malik S, Yule DI, Disease-associated mutations in inositol 1,4,5-trisphosphate receptor subunits impair channel function. J Biol Chem. 295 (2020):18160–18178. doi: 10.1074/jbc.RA120.015683. [PubMed: 33093175]

[12]. Neumann J, Van Nieuwenhove E, Terry LE, et al. , Disrupted Ca^{2+} homeostasis and immunodeficiency in patients with functional IP_3 receptor subtype 3 defects. Cell Mol Immunol. 20 (2023):11–25. doi: 10.1038/s41423-022-00928-4. [PubMed: 36302985]

[13]. Berridge MJ, Irvine RF, Inositol trisphosphate, a novel second messenger in cellular signal transduction. Nature. 312 (1984):315–321. [PubMed: 6095092]

[14]. Burgess GM, Godfrey PP, McKinney JS, Berridge MJ, Irvine RF, Putney JW Jr., The second messenger linking receptor activation to internal Ca release in liver. Nature. 309 (1984):63–66. [PubMed: 6325926]

[15]. Yao Y, Choi J, Parker I, Quantal puffs of intracellular Ca^{2+} evoked by inositol trisphosphate in Xenopus oocytes. J Physiol. 482 (Pt 3) (1995):533–553. doi: 10.1113/jphysiol.1995.sp020538. [PubMed: 7738847]

[16]. Taufiq Ur R, Skupin A, Falcke M, Taylor CW, Clustering of InsP3 receptors by InsP3 retunes their regulation by $InsP_3$ and Ca^{2+}. Nature. 458 (2009):655–659. doi: 10.1038/nature07763. [PubMed: 19348050]

[17]. Smith IF, Wiltgen SM, Shuai J, Parker I, Ca^{2+} puffs originate from preestablished stable clusters of inositol trisphosphate receptors. Sci Signal. 2 (2009):ra77. doi: 10.1126/scisignal.2000466. [PubMed: 19934435]

[18]. Shen Y, Thillaiappan NB, Taylor CW, The store-operated Ca^{2+} entry complex comprises a small cluster of STIM1 associated with one Orai1 channel. Proc Natl Acad Sci U S A. 118 (2021). doi: 10.1073/pnas.2010789118.

[19]. Lock JT, Alzayady KJ, Yule DI, Parker I, All three IP_3 receptor isoforms generate Ca^{2+} puffs that display similar characteristics. Sci Signal. 11 (2018). doi: 10.1126/scisignal.aau0344.

[20]. Mataragka S, Taylor CW, All three IP_3 receptor subtypes generate Ca^{2+} puffs, the universal building blocks of IP_3-evoked Ca^{2+} signals. J Cell Sci. 131 (2018). doi: 10.1242/jcs.220848.

[21]. Patel S, Marchant JS, Brailoiu E, Two-pore channels: Regulation by NAADP and customized roles in triggering calcium signals. Cell Calcium. 47 (2010):480–490. doi: 10.1016/j.ceca.2010.05.001. [PubMed: 20621760]

[22]. Atakpa-Adaji P, Thillaiappan NB, Taylor CW, IP_3 receptors and their intimate liaisons. Curr Opin Phisiol. 17 (2020):9–16.

[23]. Alzayady KJ, Wang L, Chandrasekhar R, Wagner LE 2nd, Petegem F. Van, Yule DI, Defining the stoichiometry of inositol 1,4,5-trisphosphate binding required to initiate Ca^{2+} release. Sci Signal. 9 (2016):ra35. doi: 10.1126/scisignal.aad6281. [PubMed: 27048566]

[24]. Prole DL, Taylor CW, Inositol 1,4,5-trisphosphate receptors and their protein partners as signalling hubs. J Physiol. (2016). doi: 10.1113/JP271139.

[25]. Foskett JK, White C, Cheung KH, Mak DO, Inositol trisphosphate receptor Ca^{2+} release channels. Physiol Rev. 87 (2007):593–658. [PubMed: 17429043]

[26]. Arige V, Yule DI, Spatial and temporal crosstalk between the cAMP and Ca^{2+} signaling systems. Biochim Biophys Acta Mol Cell Res. 1869 (2022):119293. doi: 10.1016/j.bbamcr.2022.119293. [PubMed: 35588944]

[27]. Jiang QX, Thrower EC, Chester DW, Ehrlich BE, Sigworth FJ, Three-dimensional structure of the type 1 inositol 1,4,5-trisphosphate receptor at 24 Å resolution. Embo J. 21 (2002):3575–3581. [PubMed: 12110570]

[28]. da Fonseca PC, Morris SA, Nerou EP, Taylor CW, Morris EP, Domain organization of the type 1 inositol 1,4,5-trisphosphate receptor as revealed by single-particle analysis. Proc Natl Acad Sci U S A. 100 (2003):3936–3941. [PubMed: 12651956]

[29]. Hamada K, Terauchi A, Mikoshiba K, Three-dimensional rearrangements within inositol 1, 4, 5-trisphosphate receptor by calcium. J Biol Chem. 278 (2003):52881–52889. [PubMed: 14593123]

[30]. Serysheva II, Bare DJ, Ludtke SJ, Kettlun CS, Chiu W, Mignery GA, Structure of the type 1 inositol 1,4,5-trisphosphate receptor revealed by electron cryomicroscopy. J Biol Chem. 278 (2003):21319–21322. [PubMed: 12714606]

[31]. Sato C, Hamada K, Ogura T, et al. , Inositol 1,4,5-trisphosphate receptor contains multiple cavities and L-shaped ligand-binding domains. J Mol Biol. 336 (2004):155–164. [PubMed: 14741211]

[32]. Ludtke SJ, Tran TP, Ngo QT, Moiseenkova-Bell VY, Chiu W, Serysheva II, Flexible architecture of IP3R1 by Cryo-EM. Structure. 19 (2011):1192–1199. doi: 10.1016/j.str.2011.05.003. [PubMed: 21827954]

[33]. Murray SC, Flanagan J, Popova OB, Chiu W, Ludtke SJ, Serysheva II, Validation of cryo-EM structure of IP(3)R1 channel. Structure. 21 (2013):900–909. doi: 10.1016/j.str.2013.04.016. [PubMed: 23707684]

[34]. Fan G, Baker ML, Wang Z, et al. , Gating machinery of $InsP_3R$ channels revealed by electron cryomicroscopy. Nature. 527 (2015):336–341. doi: 10.1038/nature15249. [PubMed: 26458101]

[35]. Fan G, Baker MR, Wang Z, et al. , Cryo-EM reveals ligand induced allostery underlying $InsP_3R$ channel gating. Cell Res. 28 (2018):1158–1170. doi: 10.1038/s41422-018-0108-5. [PubMed: 30470765]

[36]. Baker MR, Fan G, Seryshev AB, Agosto MA, Baker ML, Serysheva II, Cryo-EM structure of type 1 IP_3R channel in a lipid bilayer. Commun Biol. 4 (2021):625. doi: 10.1038/s42003-021-02156-4. [PubMed: 34035440]

[37]. Fan G, Baker MR, Terry LE, et al. , Conformational motions and ligand-binding underlying gating and regulation in IP_3R channel. Nat Commun. 13 (2022):6942. doi: 10.1038/s41467-022-34574-1. [PubMed: 36376291]

[38]. Paknejad N, Hite RK, Structural basis for the regulation of inositol trisphosphate receptors by Ca^{2+} and IP_3. Nat Struct Mol Biol. 25 (2018):660–668. doi: 10.1038/s41594-018-0089-6. [PubMed: 30013099]

[39]. Azumaya CM, Linton EA, Risener CJ, Nakagawa T, Karakas E, Cryo-EM structure of human type-3 inositol triphosphate receptor reveals the presence of a self-binding peptide that acts as an antagonist. J Biol Chem. 295 (2020):1743–1753. doi: 10.1074/jbc.RA119.011570. [PubMed: 31915246]

[40]. Schmitz EA, Takahashi H, Karakas E, Structural basis for activation and gating of IP3 receptors. Nat Commun. 13 (2022):1408. doi: 10.1038/s41467-022-29073-2. [PubMed: 35301323]

[41]. Serysheva II, Baker MR, Fan G: Structural Insights into IP3R fucntion. In Membrane Dynamics and Calcium Signaling. Advances in Experimental Medicine and Biology Edited by Krebs J: Springer; 2018. vol 981.]

[42]. Callaway E, The revolution will not be crystallized: a new method sweeps through structural biology. Nature. 525 (2015):172–174. doi: 10.1038/525172a. [PubMed: 26354465]

[43]. Ando H, Hirose M, Mikoshiba K, Aberrant IP(3) receptor activities revealed by comprehensive analysis of pathological mutations causing spinocerebellar ataxia 29. Proc Natl Acad Sci U S A. 115 (2018):12259–12264. doi: 10.1073/pnas.1811129115. [PubMed: 30429331]

[44]. Bosanac I, Alattia JR, Mal TK, et al. , Structure of the inositol 1,4,5-trisphosphate receptor binding core in complex with its ligand. Nature. 420 (2002):696–700. [PubMed: 12442173]

[45]. Lin CC, Baek K, Lu Z, Apo and InsP-bound crystal structures of the ligand-binding domain of an InsP receptor. Nat Struct Mol Biol. 18 (2011):1172–1174. [PubMed: 21892169]

[46]. Seo MD, Velamakanni S, Ishiyama N, et al. , Structural and functional conservation of key domains in InsP3 and ryanodine receptors. Nature. 483 (2012):108–112. doi: 10.1038/nature10751. [PubMed: 22286060]

[47]. Uchida K, Miyauchi H, Furuichi T, Michikawa T, Mikoshiba K, Critical regions for activation gating of the inositol 1,4,5-trisphosphate receptor. J Biol Chem. 278 (2003):16551–16560. [PubMed: 12621039]

[48]. Yamazaki H, Chan J, Ikura M, Michikawa T, Mikoshiba K, Tyr-167/Trp-168 in type 1/3 inositol 1,4,5-trisphosphate receptor mediates functional coupling between ligand binding and channel opening. J Biol Chem. 285 (2010):36081–36091. [PubMed: 20813840]

[49]. Baker MR, Fan G, Serysheva II, Structure of IP3R channel: high-resolution insights from cryo-EM. Curr Opin Struct Biol. 46 (2017):38–47. doi: 10.1016/j.sbi.2017.05.014. [PubMed: 28618351]

[50]. Baker ML, Serysheva II, Sencer S, et al. , The skeletal muscle Ca^{2+} release channel has an oxidoreductase-like domain. Proc Natl Acad Sci U S A. 99 (2002):12155–12160. doi: 10.1073/pnas.182058899. [PubMed: 12218169]

[51]. Klar J, Hisatsune C, Baig SM, et al. , Abolished $InsP_3R2$ function inhibits sweat secretion in both humans and mice. J Clin Invest. 124 (2014):4773–4780. doi: 10.1172/JCI70720. [PubMed: 25329695]

[52]. Schug ZT, Joseph SK, The role of the S4-S5 linker and C-terminal tail in inositol 1,4,5-trisphosphate receptor function. J Biol Chem. 281 (2006):24431–24440. [PubMed: 16815846]

[53]. Jumper J, Evans R, Pritzel A, et al. , Highly accurate protein structure prediction with AlphaFold. Nature. 596 (2021):583–589. doi: 10.1038/s41586-021-03819-2. [PubMed: 34265844]

[54]. Iino M, Biphasic Ca^{2+} dependence of inositol 1,4,5-trisphosphate-induced calcium release in smooth muscle cells of the guinea pig taenia caeci. J Gen Physiol. 95 (1990):1103–1122. [PubMed: 2373998]

[55]. Bezprozvanny I, Watras J, Ehrlich BE, Bell-shaped calcium-response curves of Ins(1,4,5)P_3- and calcium-gated channels from endoplasmic reticulum of cerebellum. Nature. 351 (1991):751–754. [PubMed: 1648178]

[56]. Marshall IC, Taylor CW, Biphasic effects of cytosolic Ca2+ on Ins(1,4,5)P3-stimulated Ca^{2+} mobilization in hepatocytes. J Biol Chem. 268 (1993):13214–13220. [PubMed: 8514760]

[57]. Marshall IC, Taylor CW, Two calcium-binding sites mediate the interconversion of liver inositol 1,4,5-trisphosphate receptors between three conformational states. Biochem J. 301 (1994):591–598. [PubMed: 8043006]

[58]. Taylor CW, Tovey SC, IP_3 receptors: toward understanding their activation. Cold Spring Harb Perspect Biol. 2 (2010):a004010. doi: 10.1101/cshperspect.a004010. [PubMed: 20980441]

[59]. Mayrleitner M, Schafer R, Fleischer S, IP3 receptor purified from liver plasma membrane is an (1,4,5)IP_3 activated and (1,3,4,5)IP_4 inhibited calcium permeable ion channel. Cell Calcium. 17 (1995):141–153. doi: 10.1016/0143-4160(95)90083-7. [PubMed: 7736563]

[60]. Arige V, Terry LE, Wagner LE 2nd et al. , Functional determination of calcium-binding sites required for the activation of inositol 1,4,5-trisphosphate receptors. Proc Natl Acad Sci U S A. 119 (2022):e2209267119. doi: 10.1073/pnas.2209267119. [PubMed: 36122240]

[61]. Bosanac I, Michikawa T, Mikoshiba K, Ikura M, Structural insights into the regulatory mechanism of IP_3 receptor. Biochim Biophys Acta. 1742 (2004):89–102. doi: 10.1016/j.bbamcr.2004.09.016. [PubMed: 15590059]

[62]. Murayama T, Ogawa H, Kurebayashi N, Ohno S, Horie M, Sakurai T, A tryptophan residue in the caffeine-binding site of the ryanodine receptor regulates Ca^{2+} sensitivity. Commun Biol. 1 (2018):98. doi: 10.1038/s42003-018-0103-x. [PubMed: 30271978]

[63]. Medeiros-Domingo A, Bhuiyan ZA, Tester DJ, et al. , The RYR2-encoded ryanodine receptor/calcium release channel in patients diagnosed previously with either catecholaminergic polymorphic ventricular tachycardia or genotype negative, exercise-induced long QT syndrome: a comprehensive open reading frame mutational analysis. J Am Coll Cardiol. 54 (2009):2065–2074. doi: 10.1016/j.jacc.2009.08.022. [PubMed: 19926015]

[64]. Chirasani VR, Xu L, Addis HG, et al. , A central core disease mutation in the Ca^{2+}-binding site of skeletal muscle ryanodine receptor impairs single-channel regulation. Am J Physiol Cell Physiol. 317 (2019):C358–C365. doi: 10.1152/ajpcell.00052.2019. [PubMed: 31166712]

[65]. Mak D-O, McBride S, Foskett JK, Inositol 1,4,5-triphosphate activation of inositol triphosphate receptor Ca^{2+} channel by ligand tuning of Ca^{2+} inhibition. Proceedings of the National Academy of Science. 95 (1998):15821–15825.

[66]. Mak DO, McBride S, Foskett JK, Regulation by Ca^{2+} and Inositol 1,4,5-Trisphosphate (InsP(3)) of Single Recombinant Type 3 $InsP_3$ Receptor Channels. Ca($^{2+}$) activation uniquely distinguishes types 1 and 3 $insP_3$ receptors. J Gen Physiol. 117 (2001):435–446. [PubMed: 11331354]

[67]. Mak DO, McBride SM, Petrenko NB, Foskett JK, Novel regulation of calcium inhibition of the inositol 1,4,5-trisphosphate receptor calcium-release channel. J Gen Physiol. 122 (2003):569–581. [PubMed: 14581583]

[68]. Tu H, Nosyreva E, Miyakawa T, et al. , Functional and biochemical analysis of the type 1 inositol (1,4,5)-trisphosphate receptor calcium sensor. Biophys J. 85 (2003):290–299. [PubMed: 12829484]

[69]. Miyakawa T, Mizushima A, Hirose K, et al. , Ca^{2+}-sensor region of IP_3 receptor controls intracellular Ca^{2+} signaling. Embo J. 20 (2001):1674–1680. [PubMed: 11285231]

[70]. Xu L, Chirasani VR, Carter JS, et al. , Ca^{2+}-mediated activation of the skeletal-muscle ryanodine receptor ion channel. J Biol Chem. 293 (2018):19501–19509. doi: 10.1074/jbc.RA118.004453. [PubMed: 30341173]

[71]. Ferris CD, Huganir RL, Snyder SH, Calcium flux mediated by purified inositol 1,4,5-trisphosphate receptor in reconstituted lipid vesicles is allosterically regulated by adenine nucleotides. Proc Natl Acad Sci U S A. 87 (1990):2147–2151. [PubMed: 2156262]

[72]. Bezprozvanny I, Ehrlich BE, ATP modulates the function of inositol 1,4,5-trisphosphate-gated channels at two sites. Neuron. 10 (1993):1175–1184. [PubMed: 7686381]

[73]. Iino M, Effects of adenine nucleotides on inositol 1,4,5-trisphosphate-induced calcium release in vascular smooth muscle cells. J Gen Physiol. 98 (1991):681–698. doi: 10.1085/jgp.98.4.681. [PubMed: 1660060]

[74]. Mak DO, McBride S, Foskett JK, ATP regulation of type 1 inositol 1,4,5-trisphosphate receptor channel gating by allosteric tuning of Ca^{2+} activation. J Biol Chem. 274 (1999):22231–22237. [PubMed: 10428789]

[75]. Arruda AP, Pers BM, Parlakgul G, Guney E, Inouye K, Hotamisligil GS, Chronic enrichment of hepatic endoplasmic reticulum-mitochondria contact leads to mitochondrial dysfunction in obesity. Nat Med. 20 (2014):1427–1435. doi: 10.1038/nm.3735. [PubMed: 25419710]

[76]. Katona M, Bartok A, Nichtova Z, et al. , Capture at the ER-mitochondrial contacts licenses IP_3 receptors to stimulate local Ca^{2+} transfer and oxidative metabolism. Nat Commun. 13 (2022):6779. doi: 10.1038/s41467-022-34365-8. [PubMed: 36351901]

[77]. Bartok A, Weaver D, Golenar T, et al. , IP(3) receptor isoforms differently regulate ER-mitochondrial contacts and local calcium transfer. Nat Commun. 10 (2019):3726. doi: 10.1038/s41467-019-11646-3. [PubMed: 31427578]

[78]. Ferris CD, Snyder SH, Inositol 1,4,5-trisphosphate-activated calcium channels. Annu Rev Physiol. 54 (1992):469–488. doi: 10.1146/annurev.ph.54.030192.002345. [PubMed: 1314042]

[79]. Furuichi T, Yoshikawa S, Miyawaki A, Wada K, Maeda N, Mikoshiba K, Primary structure and functional expression of the inositol 1,4,5- trisphosphate-binding protein P400. Nature. 342 (1989):32–38. [PubMed: 2554142]

[80]. Wagner LE 2nd, Betzenhauser MJ, Yule DI, ATP binding to a unique site in the type-1 S2-inositol 1,4,5-trisphosphate receptor defines susceptibility to phosphorylation by protein kinase A. J Biol Chem. 281 (2006):17410–17419. doi: 10.1074/jbc.M601340200. [PubMed: 16621795]

[81]. Maeda N, Kawasaki T, Nakade S, et al. , Structural and functional characterization of inositol 1,4,5- trisphosphate receptor channel from mouse cerebellum. J Biol Chem. 266 (1991):1109–1116. [PubMed: 1845986]

[82]. Mak DO, Foskett JK, Inositol 1,4,5-trisphosphate receptors in the endoplasmic reticulum: A single-channel point of view. Cell Calcium. 58 (2015):67–78. doi: 10.1016/j.ceca.2014.12.008. [PubMed: 25555684]

[83]. Yuan Q, Dridi H, Clarke OB, et al. , RyR1-related myopathy mutations in ATP and calcium binding sites impair channel regulation. Acta Neuropathol Commun. 9 (2021):186. doi: 10.1186/s40478-021-01287-3. [PubMed: 34809703]

[84]. Peng W, Shen H, Wu J, et al. , Structural basis for the gating mechanism of the type 2 ryanodine receptor RyR2. Science. 354 (2016). doi: 10.1126/science.aah5324.

[85]. Reilly-O'Donnell B, Robertson GB, Karumbi A, et al. , Dysregulated Zn^{2+} homeostasis impairs cardiac type-2 ryanodine receptor and mitsugumin 23 functions, leading to sarcoplasmic reticulum Ca^{2+} leakage. J Biol Chem. 292 (2017):13361–13373. doi: 10.1074/jbc.M117.781708. [PubMed: 28630041]

[86]. Dashti A, Mashayekhi G, Shekhar M, et al. , Retrieving functional pathways of biomolecules from single-particle snapshots. Nat Commun. 11 (2020):4734. doi: 10.1038/s41467-020-18403-x. [PubMed: 32948759]

[87]. Chen M, Ludtke SJ, Deep learning-based mixed-dimensional Gaussian mixture model for characterizing variability in cryo-EM. Nat Methods. 18 (2021):930–936. doi: 10.1038/s41592-021-01220-5. [PubMed: 34326541]

[88]. Zhong ED, Bepler T, Berger B, Davis JH, CryoDRGN: reconstruction of heterogeneous cryo-EM structures using neural networks. Nat Methods. 18 (2021):176–185. doi: 10.1038/s41592-020-01049-4. [PubMed: 33542510]

[89]. Punjani A, Fleet DJ, 3D variability analysis: Resolving continuous flexibility and discrete heterogeneity from single particle cryo-EM. J Struct Biol. 213 (2021):107702. doi: 10.1016/j.jsb.2021.107702. [PubMed: 33582281]

[90]. Punjani A, Fleet D, 3D Flexible Refinement: Structure and Motion of Flexible Proteins from Cryo-EM. Microscopy and Microanalysis. 28 (2022):1218-1218. doi: 10.1017/s1431927622005074.

[91]. Ludtke SJ, Baldwin PR, Chiu W, EMAN: semiautomated software for high-resolution single-particle reconstructions. J Struct Biol. 128 (1999):82–97. doi: 10.1006/jsbi.1999.4174. [PubMed: 10600563]

[92]. Punjani A, Rubinstein JL, Fleet DJ, Brubaker MA, cryoSPARC: algorithms for rapid unsupervised cryo-EM structure determination. Nat Methods. 14 (2017):290–296. doi: 10.1038/nmeth.4169. [PubMed: 28165473]

[93]. Zivanov J, Nakane T, Forsberg BO, et al. , New tools for automated high-resolution cryo-EM structure determination in RELION-3. Elife. 7 (2018). doi: 10.7554/eLife.42166.

[94]. Frank J, Ourmazd A, Continuous changes in structure mapped by manifold embedding of single-particle data in cryo-EM. Methods. 100 (2016):61–67. doi: 10.1016/j.ymeth.2016.02.007. [PubMed: 26884261]

[95]. Mikoshiba K, IP_3 receptor/Ca^{2+} channel: from discovery to new signaling concepts. J Neurochem. 102 (2007):1426–1446. [PubMed: 17697045]

[96]. Berridge MJ, Fain JN, Inhibition of phosphatidylinositol synthesis and the inactivation of calcium entry after prolonged exposure of the blowfly salivary gland to 5-hydroxytryptamine. Biochem J. 178 (1979):59–69. [PubMed: 435285]

[97]. Iino M, Calcium dependent inositol trisphosphate-induced calcium release in the guinea-pig taenia caeci. Biochem Biophys Res Commun. 142 (1987):47–52. [PubMed: 3493000]

[98]. Ehrlich BE, Watras J, Inositol 1,4,5-trisphosphate activates a channel from smooth muscle sarcoplasmic reticulum. Nature. 336 (1988):583–586. doi: 10.1038/336583a0. [PubMed: 2849060]

[99]. Ferris CD, Huganir RL, Supattapone S, Snyder SH, Purified inositol 1,4,5-trisphosphate receptor mediates calcium flux in reconstituted lipid vesicles. Nature. 342 (1989):87–89. [PubMed: 2554143]

[100]. Mignery GA, Sudhof TC, Takei K, De Camilli P, Putative receptor for inositol 1,4,5-trisphosphate similar to ryanodine receptor. Nature. 342 (1989):192–195. [PubMed: 2554146]

[101]. Chadwick CC, Saito A, Fleischer S, Isolation and characteriztion of the inositol triphosphate receptor from smooth muscle. Proceedings of the National Academy of Science. 87 (1990):2132–2136.

Highlights

- The intrinsically flexible 3D architecture of IP_3R provides the premise behind the multi-modal allosteric regulation of its activity
- Ligand binding alters the entropic neighborhood of conformations naturally explored by IP_3R channels
- IP_3 binding to IP_3R relies on conformational dynamics of the ARM2 domain and is based on the conformational selection of the binding pocket
- Isoform-specific affinity of IP_3Rs might be defined by the characteristic motions of the ARM2 and the correlated flexibility of LBDs
- Binding of IP_3 primes IP_3R to endow it with a capacity to respond to Ca^{2+} which then evokes channel opening
- Binding of Ca^{2+} alters the conformational landscape of IP_3R protein to exert its biphasic functional effect.
- Ligand-evoked signals are transmitted towards the channel pore via allosteric nexus connecting the CY and TM domains

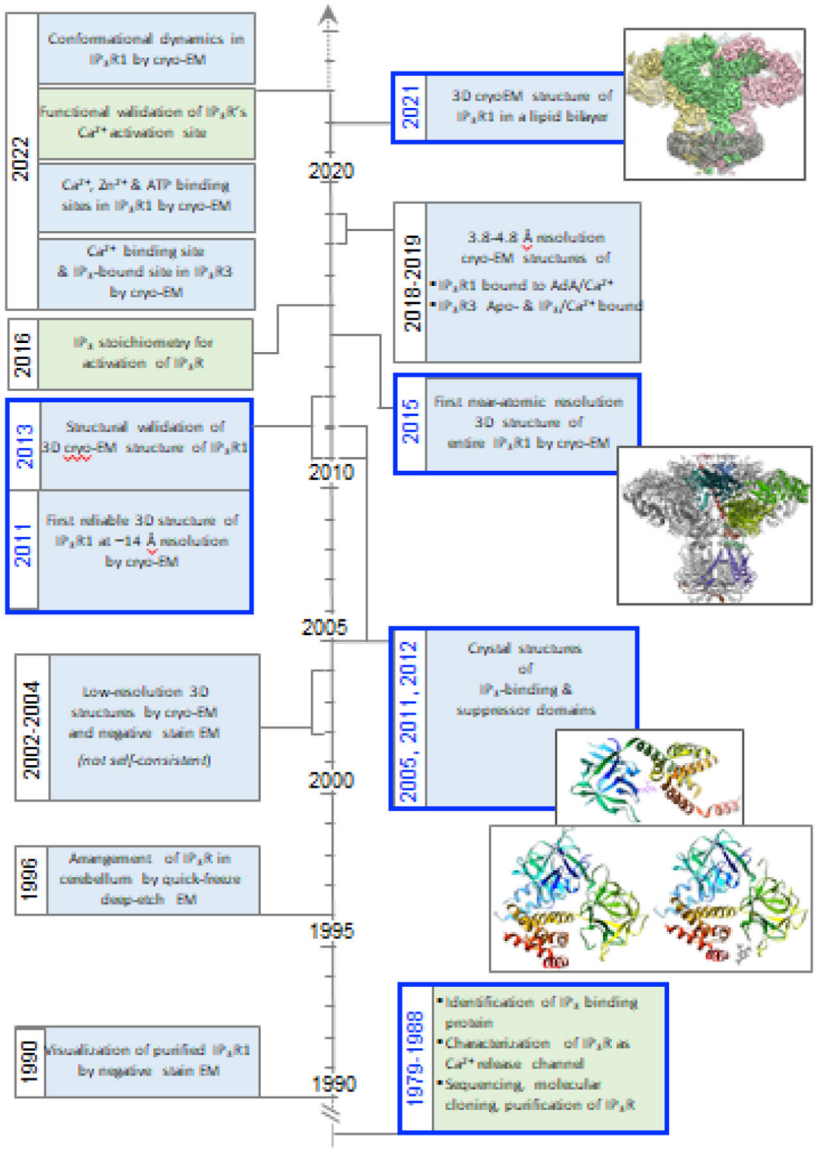

Fig. 1. Milestones toward the structure of IP_3Rs.

Paving the road for understanding the molecular mechanism underlying IP_3 receptor function began with several foundational studies that described increased intracellular Ca^{2+} mobilization by receptor-activated hydrolysis of PIP_2 [96]; stimulation of Ca^{2+} release from intracellular stores by the secondary messenger molecule IP_3; and Ca^{2+} regulation of IP_3-induced Ca^{2+} release [48,97]. Subsequently, the molecular identification of IP_3R was uncovered by purification of the IP_3-binding protein from the brain, its identification as a Ca^{2+} release channel through lipid vesicle reconstitution [98,99], and molecular cloning [79,100]. These studies were highly influential in shaping the next three decades of structure-function studies of IP_3Rs. The first images of purified IP_3R1 appeared by negative stain EM, and quick-freeze deep-etch EM was used to visualize the IP_3Rs in Purkinje cells [101]. Single-particle cryo-EM and negative stain EM of detergent solubilized IP_3Rs produced several low resolution (20–40 Å) structures, which unfortunately were not

self-consistent, leaving the true 3D structure of the tetrameric channel unclear [27–31]. Meanwhile, X-ray crystallography produced structures for the small expressed portions of the N-terminal ligand binding domains [44–46]. Importantly, the 3D cryo-EM structure of IP_3R1 in the closed state at ~14 Å resolution was determined and rigorously validated, thus illuminating the authentic 3D structure of IP_3R1 [32,33]. Early adoption of direct electron detectors allowed for the IP_3R channel to catch the wave of the 'resolution revolution' with the first near-atomic resolution structure of IP_3R produced by cryo-EM [34]. An outstanding question on how many IP_3 ligands are needed to bind to the tetrameric channel in order to open the gate was settled using concatenated IP_3Rs. Cryo-EM structure of IP_3R in the presence of channel activator, adenophostin A [34–37], as well as structures of the type 3 IP_3R isoform were determined by single particle cryo-EM [38–40]. Lipid-binding sites were identified in IP_3R1 by cryo-EM followed by identification of ATP, IP_3, Zn^{2+}, and Ca^{2+} binding sites. The Ca-III_S site in the ARM3 domain was determined to be the Ca^{2+} binding site for Ca^{2+} activation of IP_3R1 and IP_3R3 by mutagenesis and single-channel studies. Machine-learning analysis of cryo-EM data revealed structural dynamics of IP_3R1 controls access to IP_3 binding domains.

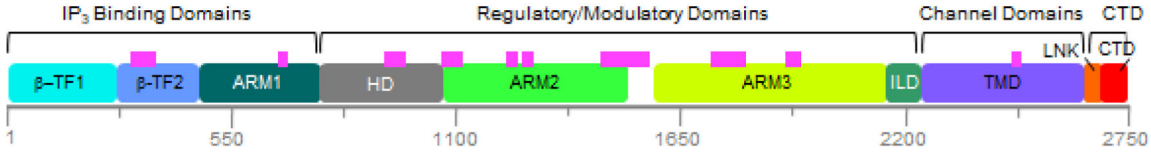

	IP_3R1	IP_3R2	IP_3R3	RyR1 homologous domains
βTF1	1-225	1-225	1-225	1-207
βTF2	226-435	226-435	226-435	208-392
ARM1	436-674	436-674	436-674	393-627
HD	693-1102	691-1102	691-1102	1657-2144
ARM2	1103-1567	1103-1582	1103-1582	2145-2617
ARM3	1582-2192	1582-2144	1582-2120	3624-4174
ILD	2193-2272	2145-2225	2121-2200	4175-4253
TMD	2273-2610	2226-2560	2201-2536	4541-4956
LNK	2611-2681	2561-2635	2537-2610	4957-5037
CTD	2682-2750	2636-2701	2611-2646	-

Fig. 2. Overall Domain Structure of IP_3Rs.

The top panel shows a linear depiction of the IP_3R1 protomer sequence showing the location of protein structural (in colored boxes) and functional domains. Magenta bars indicate unresolved regions in IP_3R structures. The lower panel lists the domain names, color coded as in the top panel, with the amino acid residues for the domain boundaries for rat IP_3R1 (P29994), human IP_3R2 (Q14571) as modeled using AlphaFold2, human IP_3R3 (Q14573) and the structurally homologous regions found in rabbit RyR1 (P11716).

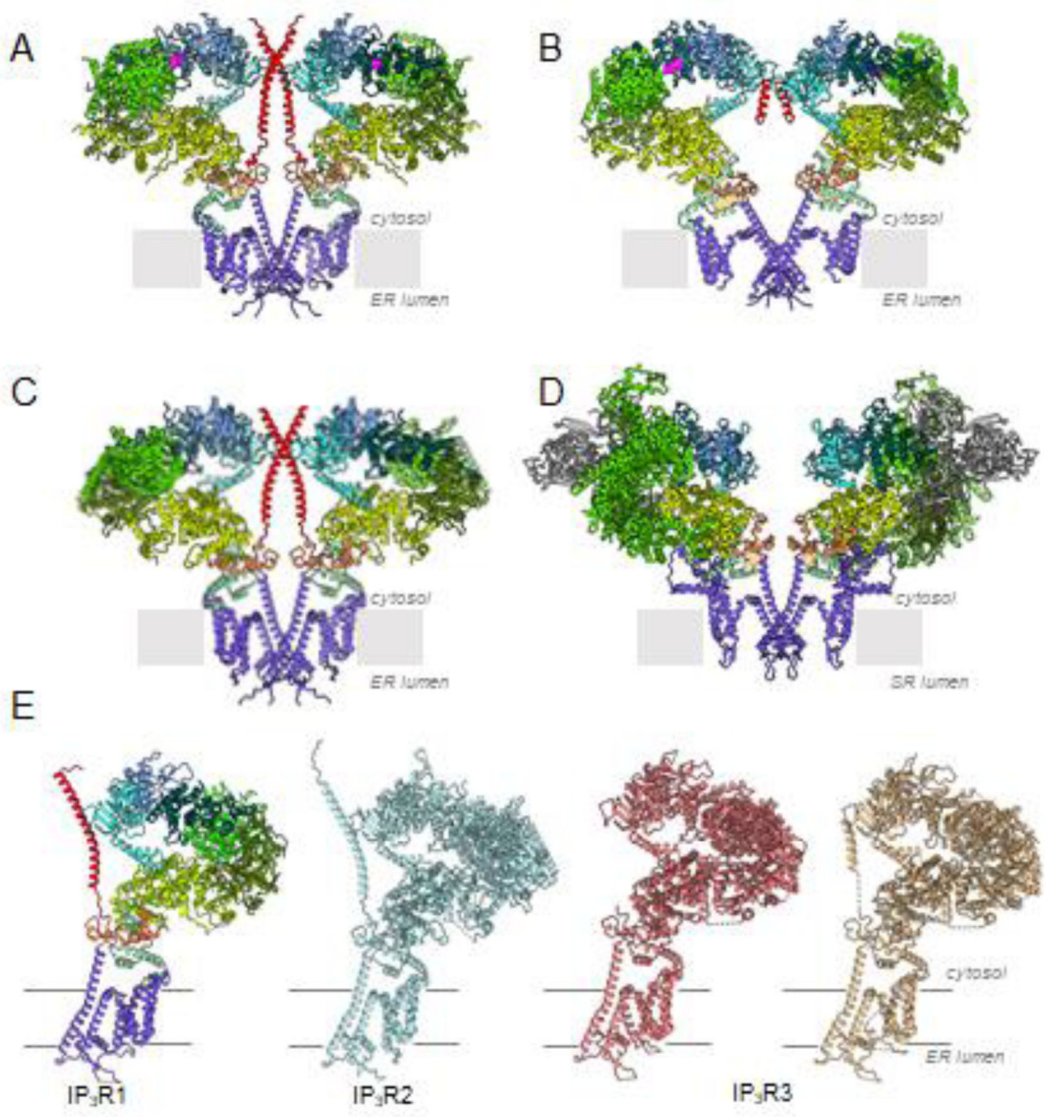

Fig. 3. Structural conservation of intracellular Ca^{2+} release channels. (A-D)

Two opposing subunits of IP_3R1 (8EAR), IP_3R3 (7T3T), IP_3R2 (AlphaFold2) and RyR1 (7M6A) viewed along the membrane plane. Domains are color-coded according to Fig. 2. Domains of RyR1 with no structure consistent with IP_3R are shown in gray. Bound IP_3 molecules are colored magenta; bound ATP is colored orange. (**E**) Structural comparison of three isoforms of IP_3R channel in ligand-free state. One subunit is shown, IP_3R1 - 7LHE, colored by domain; IP_3R2 - predicted model, light blue; IP_3R3s - 6DQJ, coral; 6UQK, tan.

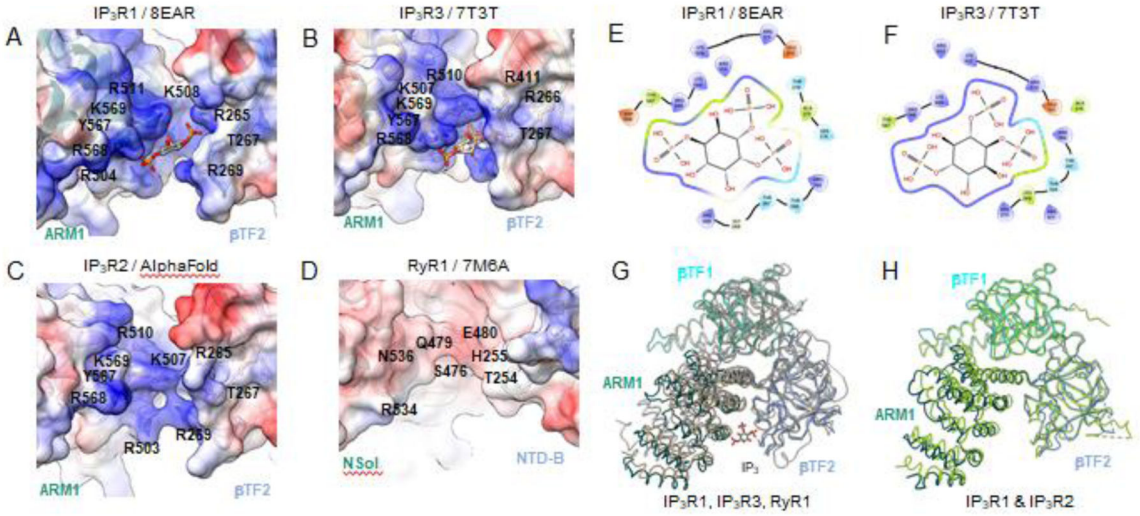

Fig. 4. Properties of the IP_3 binding pocket. (A-C)

The surface electrostatic potential in the IP_3 binding pocket of IP_3R1 (8EAR), IP_3R3 (7T3T), IP_3R2 (predicted model) with corresponding residues labeled. Blue surfaces - positive charges; red surfaces - negative charges. **(D)** Overall negative electrostatic surface potential for the cleft between RyR1 (7M6A) domains NTD-B and NSol, structurally similar to the IP_3R β-TF2 and ARM1 domains. (**E-F)** Schematic plot of the IP_3 molecule interacting with surrounding residues within the ligand-bound structure of IP_3R1 (8EAR) and IP_3R3 (7T3T). Colors indicate residue properties: green - hydrophobic; purple - positively charged; light blue - polar; red - negatively charged. **(G)** Structural alignment and overlay of the IP_3 binding pocket in IP_3R1 (8EAR, colored by domain), IP_3R3 (7T3T, tan) and RyR1 (7M6A, gray). **(H)** Structural alignment and overlay of the IP_3 binding pocket in ligand free structure of IP_3R1 (7LHE, colored by domain) and IP_3R2 (modeled with Alphafold2, light green).

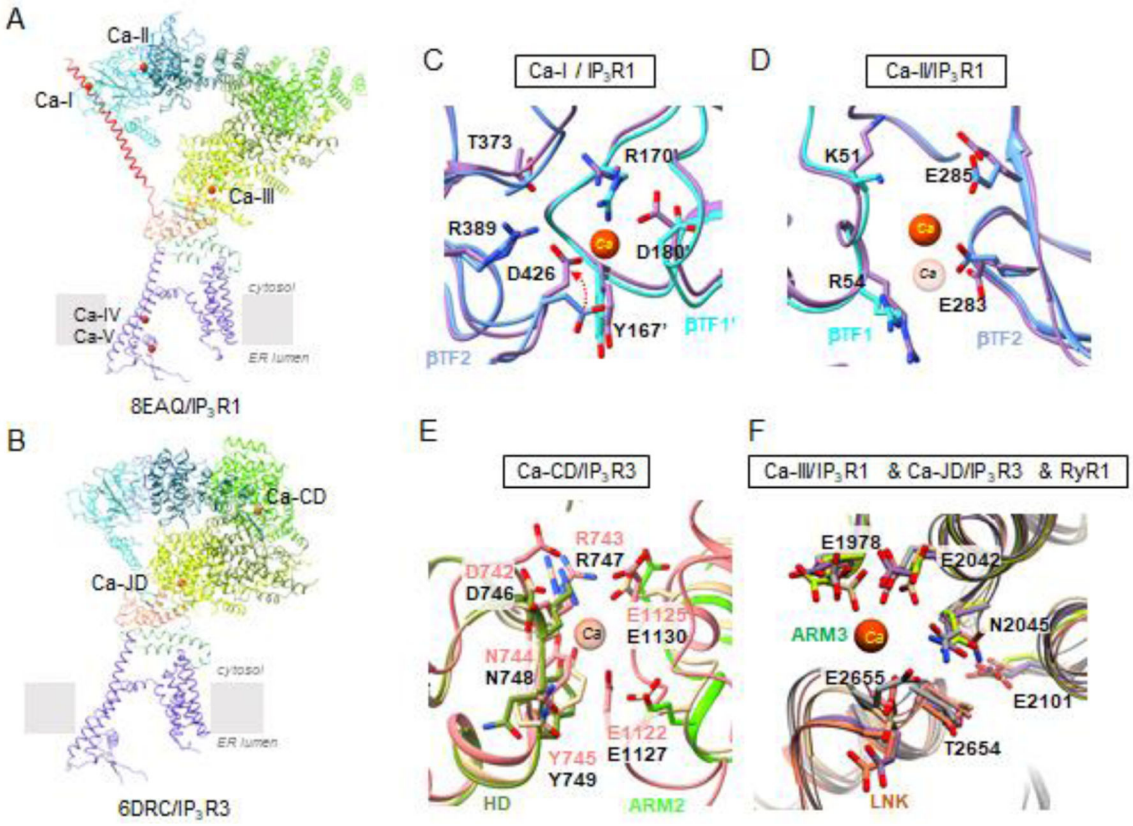

Fig. 5. Defining Ca^{2+} binding sites in IP_3Rs.

Overall topology of Ca^{2+} binding sites is shown for a single subunit of **(A)** IP_3R1 (8EAQ) and **(B)** IP_3R3 (6DRC) colored by domains as defined in Fig. 2. **(C,D)** Comparison of Ca^{2+}-binding sites identified in ligand binding domains of CIA-IP_3R1 (8EAR, colored by domain) and Ca-IP_3R1 (8EAQ, lavender): **(C)** Ca-I_{LBD}, red arrow indicates the change in side chain position of D426 contributing to loss of Ca^{2+} binding to Ca-I_{LBD} in CIA-IP_3R1; (**D)** Ca-II_{LBD}. (**E)** Structural alignment and overlay of CD-Ca binding site between IP_3R3 and IP_3R1 (IP_3R1 - 8EAR, colored by domain; IP_3R3 - 6DRC/pink, 7T3T/tan) Ca^{2+} has only been observed in 6DRC. **(F)** Structural alignment and overlay of Ca-III_S binding site in the Ca^{2+} - sensor domain for IP_3Rs and RyR1 (IP_3R1 - 8EAR, colored by domain; IP_3R3 - 6DRC, pink; 7T3T, tan; RyR1 - 7M6A, gray). Ca^{2+} ions are shown as red spheres; corresponding residues are displayed in a stick representation and labeled.

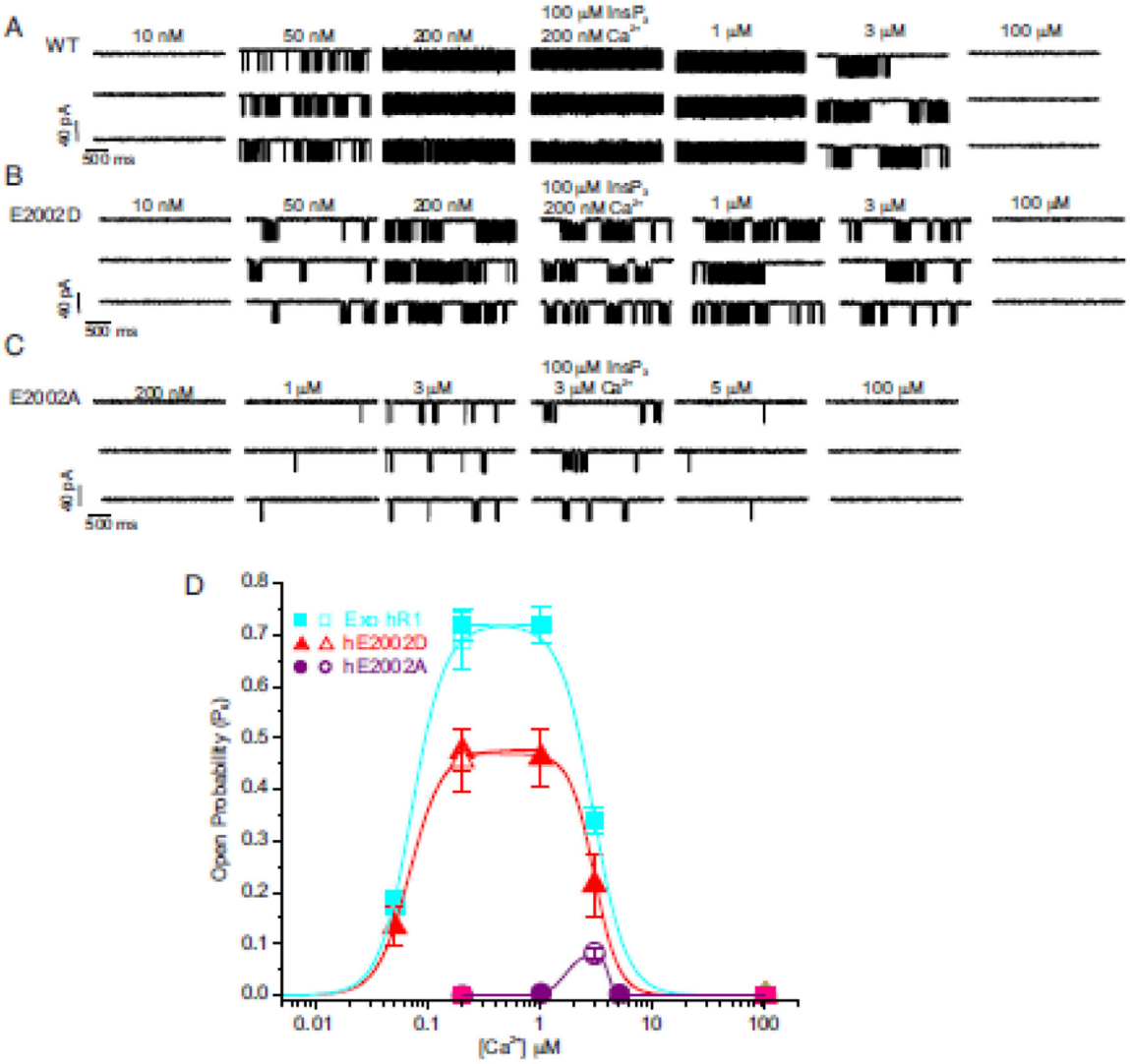

Fig. 6. Functional determination of the activating Ca^{2+} binding site in IP_3R1 and IP_3R3.

Single-channel current traces obtained using nuclear patch-clamp experiments from DT40-3KO cells stably expressing (**A**) wild-type (WT), (**B**) E2002D, and (**C**) E2002A hIP_3R1 in response to increasing $[Ca^{2+}]$ (10 nM-100 μM) at fixed concentrations of IP_3 (10 μM) (when IP_3 concentration is not indicated) and an optimal [ATP] (5 mM). The maximal open probability (P_o) for the WT and E2002D channels were obtained in the range of 0.2 to 1 μM $[Ca^{2+}]$ and diminished upon a further increase in $[Ca^{2+}]$. The P_o for E2002D remained diminished compared to WT channels at all the tested $[Ca^{2+}]$ without a notable change in Ca^{2+} dependency. The P_o of E2002A was significantly diminished when compared to either WT or E2002D and required a higher $[Ca^{2+}]$ (3 μM) for maximal P_o. The P_o remained unaltered even upon increasing the $[IP_3]$ to 100 μM at optimal $[Ca^{2+}]$ and [ATP] in all the stable cell lines (4^{th} representative trace in each panel). (**D**) Pooled data displaying diminished open probability of mutant IP_3R1 channels, biphasic effect of Ca^{2+} on IP_3R channel opening, and a clear rightward shift in the Ca^{2+}-dependency of E2002A channel compared to WT and E2002D channels. Modified from [60].

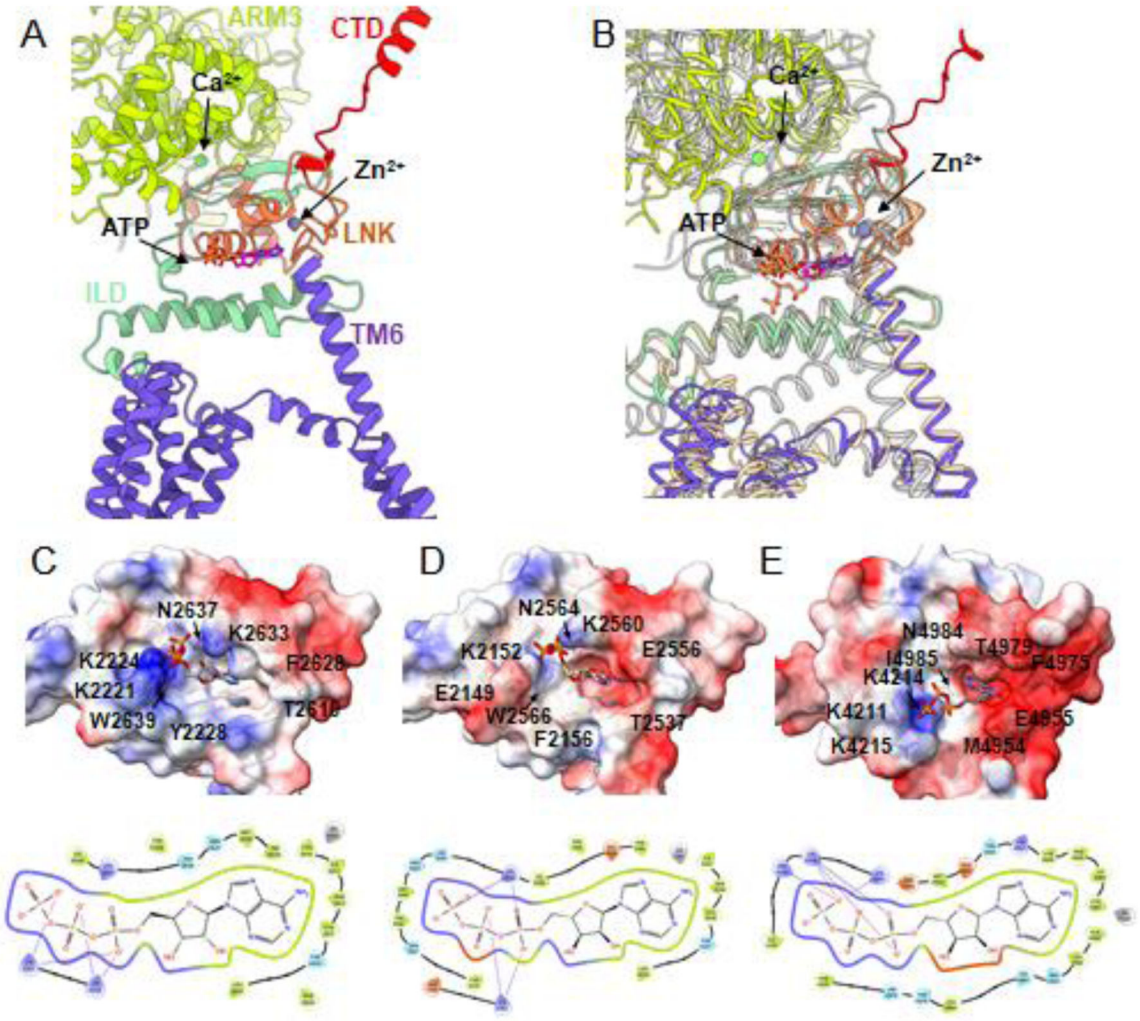

Fig. 7. Ligand binding domains within the allosteric nexus at the cytosolic–lipid bilayer interface.

(A) Zoomed-in view along the membrane plane of the domains comprising the allosteric nexus interface of one IP_3R1 subunit. IP_3R1 (8EAR) is colored by domain as defined in Fig. 2. **(B)** Structural alignment of the IP_3R1 subunit in **A** with IP_3R3 (tan; 7T3T) and RyR1 (gray; 7M6A). **(C-E)** Upper panels show the ATP binding site for **(C)** IP_3R1 (8EAR), **(D)** IP_3R3 (7T3T) and **(E)** RyR1 (7M6A) overlaid with surface electrostatic potential (blue - positive charge; red - negative charge) with several residues contributing to ligand-association labeled. Lower panels show the residues that comprise the ATP binding pocket in the above panels, respectively. Colors indicate: green - hydrophobic; purple - positively charged; light blue - polar; red - negatively charged residues, gray - zinc, lines - salt bridges.

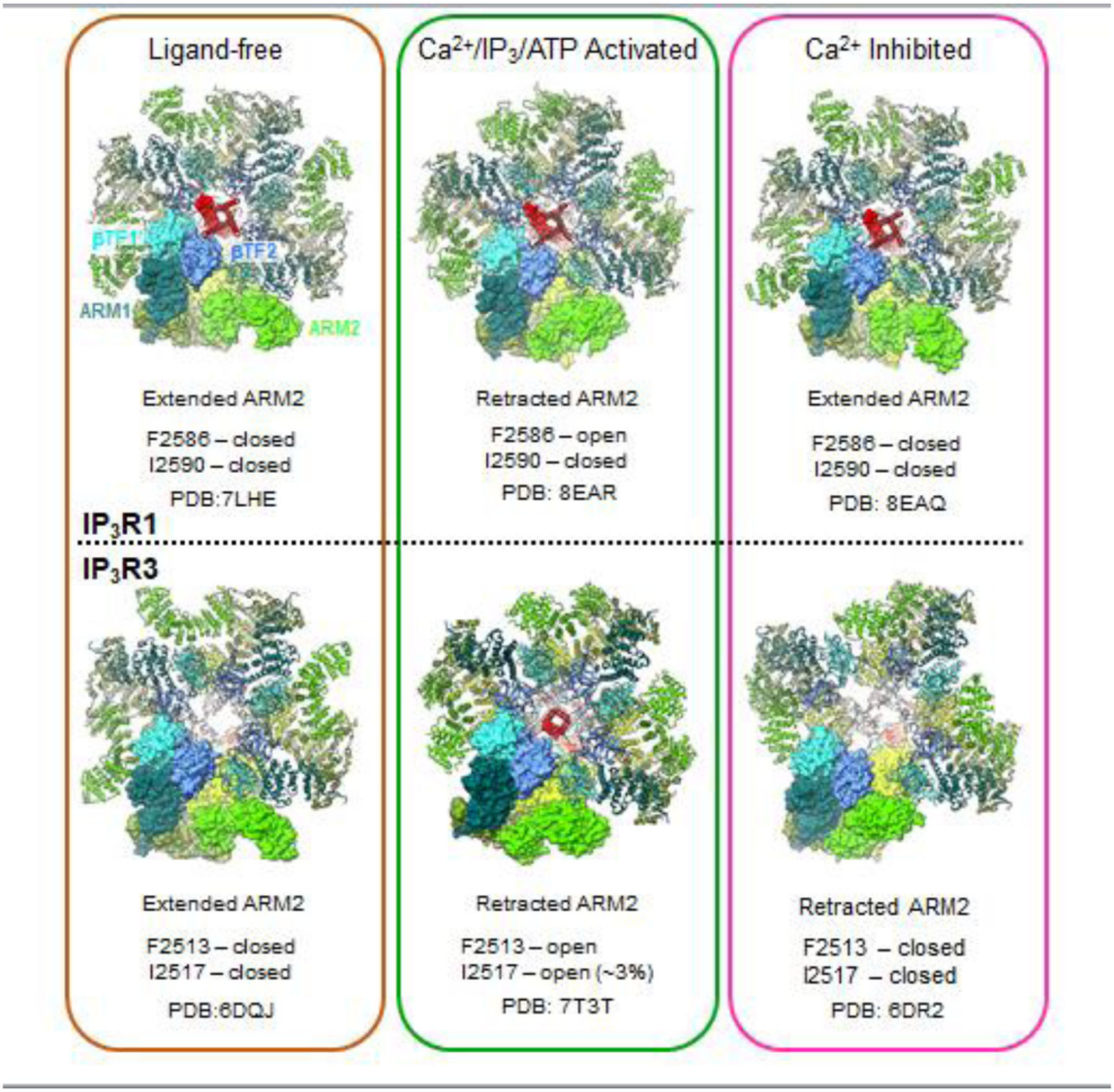

Fig. 8. ARM2 domain undergoes large conformational change

under conditions of ligand-free (left column), Ca^{2+}/IP_3/ATP activated (middle column) and high Ca^{2+} inhibited (right column). Atomic models for the tetrameric assembly of type 1 and type 3 IP_3R channel are viewed along the central four-fold axis from the cytosol with color-coded by domain, one subunit is shown with atomic surface rendering. Upper panel: IP_3R1; lower panel: IP_3R3. Conformation of ARM2 (extended or retracted) and gate (open or closed) and PDB ID are listed.

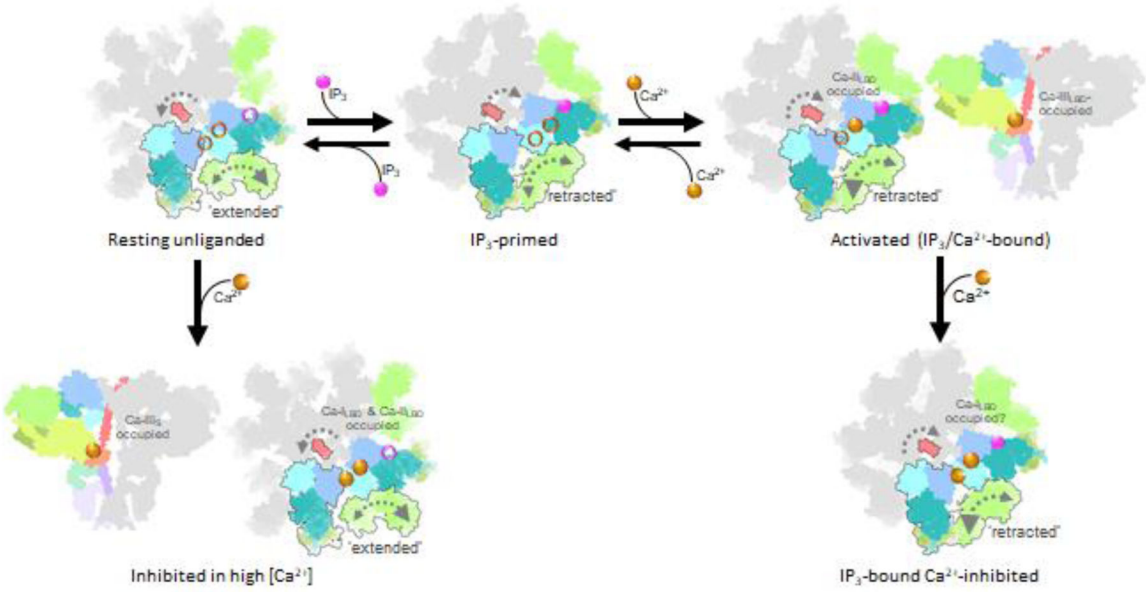

Fig. 9. Model of allosteric regulation underlying channel activation and inhibition in IP_3Rs.

IP_3Rs exhibit structural dynamics, particularly within the ARM2 domain that switches between 'extended' and 'retracted' conformations (larger gray arrowhead indicates greater amplitude of exploring the displayed conformation). Intrinsic flexibility of ARM2 domain allows for a reversible ratcheting mechanism that impacts IP_3 binding with the 'extended' conformation suitable for capturing IP_3 due to release of structural constraints at interfaces between ARM2 and βTF1' and ARM1' from the neighboring subunit. Ca^{2+} activation requires Ca^{2+} binding to the Ca-III_S in the ARM3 domain and the Ca-II_{LBD} and Ca-II_{LBD} binding site is occupied by Ca^{2+}. Ca^{2+} Inhibition of IP_3-bound-IP_3R may occur by Ca^{2+} binding to the Ca-I_{LBD} site or an additional Ca^{2+}-binding site.